2. The Setting: Overview of the Tropical Atmosphere

The tropical atmosphere is one of the last frontiers of meteorology. Formally, it is the portion of the atmosphere that lies between the Tropics of Cancer and Capricorn (23.87^o north and south, respectively), comprising 40% of the mass of the atmosphere. But in a more colloquial sense, the tropical atmosphere is loosely defined as the part of the atmosphere in which radiation, moist convection, and thermally direct overturning circulations dominate the physics. For our purposes, we will take this to include places in which shallow convection prevails beneath a region in which net radiative cooling approximately balances warming associated with large-scale subsidence. Such regions are often referred to as "sub-tropical". It is important, though, to recognize that there are no real geographic boundaries between sub-tropical and tropical regimes; indeed, in many places there is an alternation between periods of deep and shallow convection.

In coming to a conceptual understanding of complex fluid systems, it is often helpful to begin by identifying simple, often stationary, nonlinear solutions of the system and ask whether those systems are stable. If not, what is the nature of the instabilities that develop, and what kind of statistical equilibrium do they help establish?

For example, in conceptualizing the behavior of synoptic and planetary scales at middle and high latitudes, it is helpful to begin with a simple, zonally symmetric, stably stratified atmosphere with a meridional temperature gradient in thermal wind balance with a zonal wind. In the absence of friction, topography, and diabatic processes, such a state is an exact solution of the governing equations. In elementary treatments of geophysical fluid dynamics and meteorology, the processes that establish and/or maintain such states are seldom dwelled upon, and many students think of such a state simply as the time mean state of the system[1].

Disturbances to such a state are usually idealized as being inviscid and adiabatic and thus contain a set of invariant quantities, the most important of which is the potential vorticity. If the time scales of the disturbances are sufficiently long compared to the inverse of the Coriolis parameter, then the disturbances themselves are approximately in geostrophic (and hydrostatic) balance, and the potential vorticity can be inverted, subject to certain boundary conditions, to obtain the balanced flow and thermodynamic variables. The conservation and invertibility of potential vorticity offers a compact way of understanding synoptic and planetary scales phenomena at middle and high latitudes. Once can then go on to ask how these disturbances affect the mean state. Frictional and diabatic processes are usually regarded as of secondary importance.

By contrast, diabatic processes are of first-order importance of much of what happens in the tropics, and thus the tools we are accustomed to using at higher latitudes are of less utility in the tropics. In particular, it is seldom useful to regard the dynamics of tropical disturbances as adiabatic perturbations on a stably stratified background state. Even so, the concept of balance

[1] Formally, the time mean, zonal mean state of an eddy-containing atmosphere cannot be in strict thermal wind balance because of Reynold stresses in the meridional momentum equation.

applies to a surprisingly large spectrum of tropical phenomena, though in some cases the balance is nonlinear and the geostrophic approximation is poor.

Where the middle latitudes are characterized by strong horizontal temperature gradients, the tropics are relatively homogeneous, because strong temperature gradients cannot usually be maintained in the presence of small values of the Coriolis parameter. (But strong vortices can and do have strong local temperature gradients, an example of nonlinear balance.) Thus a natural starting point for the tropics is the state of radiative-convective equilibrium (RCE), in which there is a statistical equilibrium between radiation and deep moist convection and horizontal energy transport is neglected. In RCE, diabatic processes are not only non-negligible, they are central. And, unlike the case of a zonal wind in thermal wind balance, RCE is a *statistical* equilibrium state, definable only in terms of a space-time or ensemble average.

Perturbations to RCE cannot logically be considered to be dry adiabatic, and in many cases it is not consistent to neglect associated perturbations in the radiation fields. Thus the middle latitude toolbox based on conservation of dry adiabatic invariants is not usually applicable to the tropics, and the paired principle of potential vorticity invertibility, based on geostrophic balance, can only be applied to certain large-scale tropical circulations and, in modified form, to strongly-rotating local disturbances such as tropical cyclones.

But if we must discard or modify our cherished middle latitude tools, we have one or two new ones that may serve to pave a pathway to conceptual understanding of many tropical phenomena. An important one, that we shall make extensive use of throughout this book, is the principle of *convective criticality*, which holds that the deep-convecting tropical atmosphere is in a state that is nearly neutral to deep moist convection. The lack of strong horizontal gradients in the properties of the tropical atmosphere and underlying surface makes it difficult to build up large amounts of convective inhibition or the convective available potential energy (CAPE) that often goes with it, so that deep convection is much more nearly in a state of statistical equilibrium with its large-scale environment, much as dry boundary layer convection is regarded as being in equilibrium with whatever is forcing it.

In its simplest form, convective criticality implies that the (virtual) temperature profile of the deep-convective tropical atmosphere lies along some suitably defined moist adiabat. To the extent this is true, and if the motions may be considered hydrostatic, we will show that the vertical structure of the pressure field is pre-determined, placing strong constraints on the dynamics of motions that are strongly coupled to deep convection. In the limiting case of small amplitude perturbations with a rigid lid at the tropopause, the linear equations reduce to the shallow water equations.

In locally balanced flows, such as tropical cyclones, the principle of convective criticality can be generalized to a statement that the vertical temperature profile along a vortex line (or angular momentum surface of a balanced, axisymmetric vortex) of the balanced flow lies along some suitably defined moist adiabat. If such a moist adiabat can be defined by the constancy of some saturated moist entropy variable, then it follows that a potential vorticity based on that variable is zero, since the dot product of the vorticity with the gradient of that entropy vanishes. Thus, to some level of approximation, the deep-convective portions of the tropical atmosphere may be characterized as having *zero saturation potential vorticity*. This quantity is constant not because it is conserved (it isn't), but because convection forces it to vanish. Yet, under suitable balance

conditions, it is fully invertible. In this case, as in the Eady problem of baroclinic instability, all the dynamics collapses to time-dependent boundary conditions.

Thus, when we make the intellectual journey from the middle latitudes to the tropics, we must abandon some of our traditional assumptions and tools, but on the other hand we gain some new ones, and other important concepts from higher latitudes do travel, in altered form, with us. To begin this journey we must familiarize ourselves with, and indeed learn to love, the physics of radiative transfer and water so neglected in most text books on middle latitude dynamics.

2.1 Radiative transfer

Understanding how electromagnetic radiation interacts with the atmosphere, the clouds within it, and the surface is critical for understanding much of what goes on in the tropics. This text is meant to provide an overview but can be no substitute for a full treatment of the subject; it assumes that the student has some working familiarity with the physics of radiative transfer. Those wishing a more comprehensive treatment are encouraged to read the excellent text by Pierrehumbert (2010).

Let's begin by reviewing the earth's radiation budget, as determined from satellite and surface measurements of radiation and turbulent fluxes. Figure 2.1 summarizes in very broad form the fluxes of energy through the global atmosphere.

Averaged over a year and over the whole surface area of the planet, about $342\,Wm^{-2}$ of solar energy enters the "top of the atmosphere" (TOA), which can be thought of as the level below which 99.9% of the mass of the atmosphere lies. Of this, about $30\,Wm^{-2}$ (a little less than 9%) is reflected by the surface and another $77\,Wm^{-2}$ (around 22%) is backscattered to space from clouds and, to a lesser extent, aerosols and the gaseous constituents of the atmosphere itself. This yields a net planetary reflectivity (albedo) of around $107\,Wm^{-2}$ or 30%.

About $67\,Wm^{-2}$, or 20%, of the incoming solar radiation is absorbed by the atmosphere and clouds and aerosols within it. Most of the gaseous absorption in the troposphere is by water vapor, which is somewhat more abundant in the tropical atmosphere than at higher latitudes, so this percentage is higher in the tropics. This helps create a diurnal cycle in tropical weather even over deep ocean waters whose surface temperature may not have a strong diurnal cycle.

Only a little less than half ($168\,Wm^{-2}$) of the TOA solar radiation makes it to the surface, on average. The surface radiates nearly as a blackbody with a characteristic temperature, in the tropics, of around 300 Kelvins. At this temperature, most of the $460\,Wm^{-2}$ of emitted radiation (as well as the $390\,Wm^{-2}$ for the globe as a whole) is in the infrared form. Much of this is absorbed in the lower atmosphere by greenhouse gases and clouds, which also re-emit infrared radiation. In the global mean, $324\,Wm^{-2}$ are re-radiated to and absorbed the surface; this number is quite a bit larger in the tropics. This back-radiation from the atmosphere constitutes what is known in common parlance as the "greenhouse effect". Thus, again in the global mean, only about $66\,Wm^{-2}$ of the $168\,Wm^{-2}$ of incoming solar radiation at the surface is lost in the form of infrared radiation, the rest is transmitted to the atmosphere by turbulent motions in the boundary layer. Over tropical oceans, the fraction lost by infrared radiation is appreciably less,

thanks to the greater water vapor content (and thus greenhouse effect) of the atmosphere, and most of the incoming solar radiation is balanced by evaporation of ocean water.

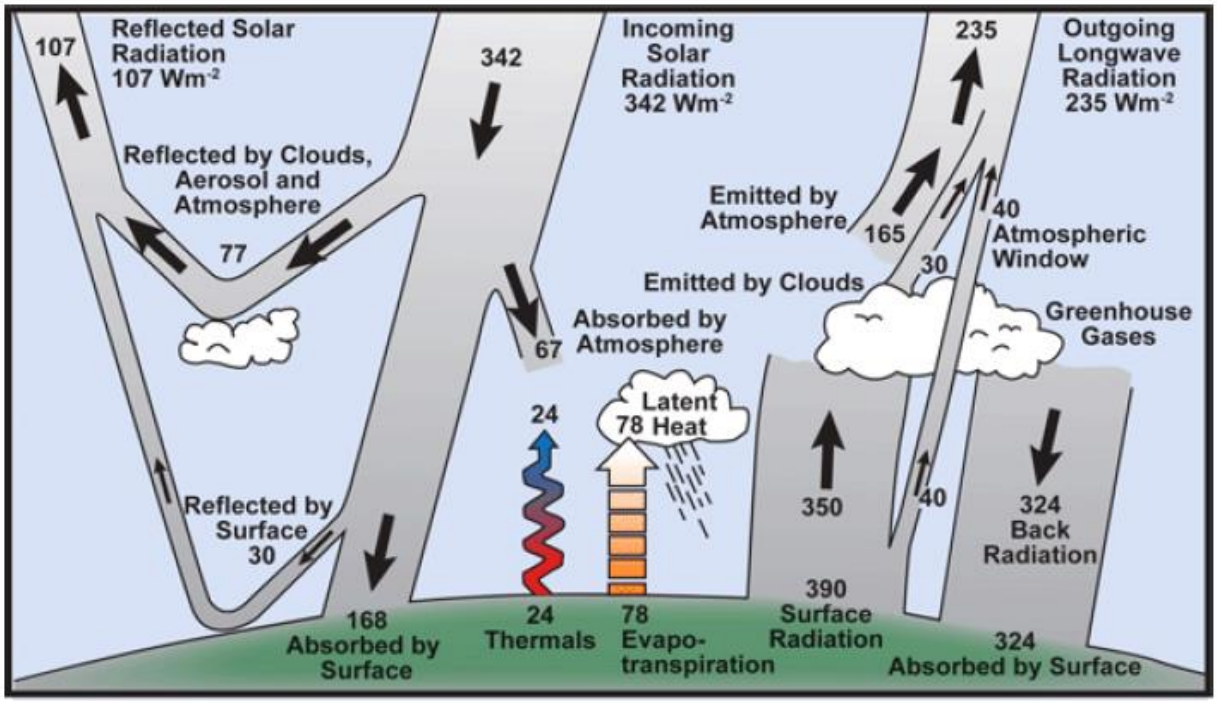

Figure 2.1: Broad overview of the earth's energy budget.

Ultimately, the earth system radiates $235\,Wm^{-2}$ back to space, in the form of mostly infrared radiation, to balance the incoming solar radiation less the fraction reflected back to space.

In its most fundamental form, radiation can be characterized by its wavelength, energy intensity at that wavelength, and its direction. In particular, the *radiant intensity,* I_λ, is the flux of energy per unit solid angle per unit wavelength of the radiation, and its relationship to the radiant flux density through a horizontal surface is illustrated in Figure 2.2. The monochromatic flux density (radiant energy flux per unit horizontal area per unit wavelength), F_λ, is given by

$$F_\lambda = \int_\Omega I_\lambda \cos\theta d\Omega, \tag{2.1}$$

where $d\Omega$ is the incremental solid angle. The total flux density (energy flux per unit horizontal area), F, is then just given by

$$F = \int_0^\infty F_\lambda d\lambda. \tag{2.2}$$

As a beam of photons of a given wavelength travels through the atmosphere, it may be partially absorbed, scattered, and added to by emissions from greenhouse gases, aerosols, and clouds. The fundamental equation governing the change of radiant intensity per unit distance, s , is

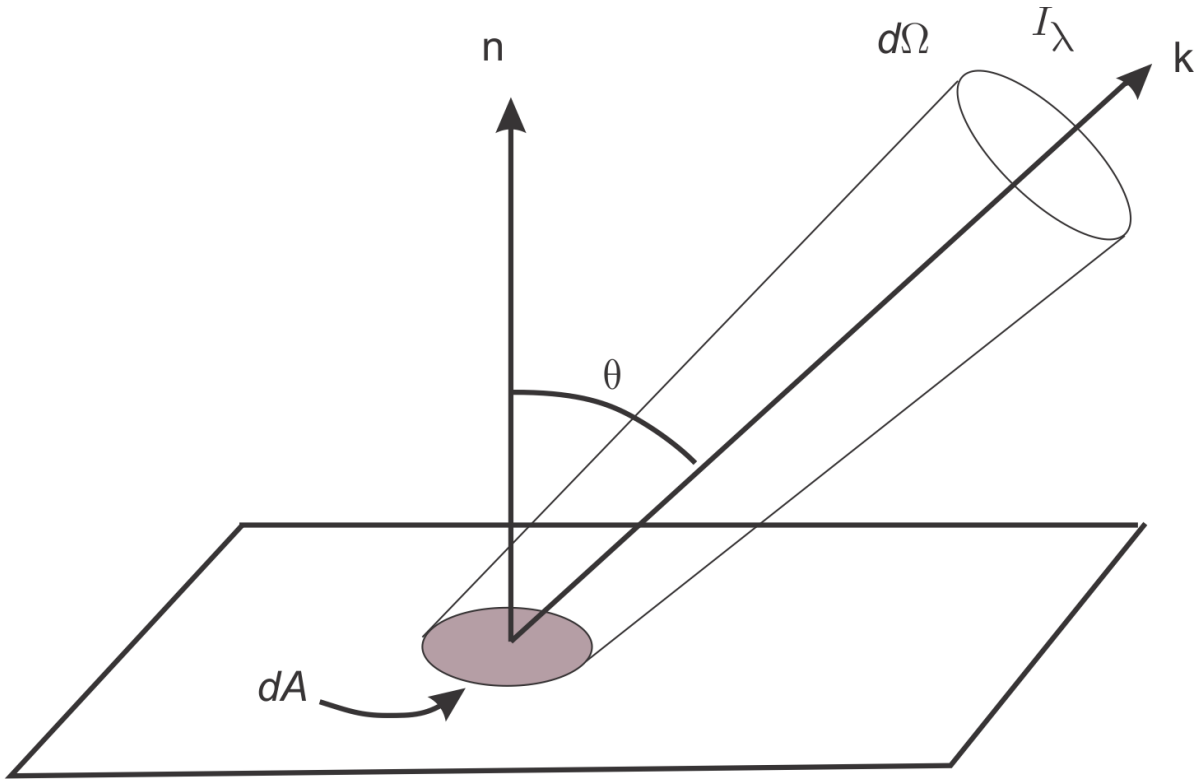

Figure 2.2: Relationship between the monochromatic flux density through a horizontal surface, the monochromatic radiant intensity, I_λ , the incremental solid angle, $d\Omega$, and the zenith angle, θ .

$$\frac{dI_\lambda}{ds} = -\left(\kappa_\lambda + \sigma_\lambda\right) I_\lambda + \varepsilon_\lambda + \beta_\lambda, \tag{2.3}$$

where κ_λ is the *absorption coefficient,* σ_λ *is* the *scattering coefficient* (both with dimensions of inverse length), ε_λ is the *emission coefficient*, and β_λ is the scattering source function.

Scattering by the gaseous constituents of the atmosphere is well approximated by Rayleigh scattering, in which the size of the scatterers (molecules of the constituents of air) is very small compared to the wave length of the radiation. This affects primarily the shortwave end of the visible spectrum through the ultraviolet and is responsible for the blue color of the sky. Scattering by clouds is more nearly in the Mie regime, where the particle sizes are comparable to the wavelengths being scattered, which includes much of the visible and slightly longer

components of the solar spectrum. Scattering of terrestrial (infrared) radiation in our atmosphere is negligible.

Provided local thermodynamic equilibrium (LTE) conditions apply, *Kirchoff's Law*, which relates emissions to blackbody radiation is valid. This can be written

$$\varepsilon_\lambda = \kappa_\lambda B_\lambda(T), \tag{2.4}$$

where $B_\lambda(T)$ is the blackbody intensity, given by *Planck's Law*:

$$B_\lambda(T) = \frac{2hc^2}{\lambda^5\left[e^{hc/\lambda kT} - 1\right]}, \tag{2.5}$$

in which h is the Planck constant, c is the speed of light, k is Boltzmann's constant, and T is the temperature. Local thermodynamic equilibrium is a good approximation for all the regions in which appreciable quantities of solar and infrared radiation are absorbed and emitted in our atmosphere. Using (2.5) allows us to write (2.3) as

$$\frac{dI_\lambda}{ds} = -\left(\kappa_\lambda + \sigma_\lambda\right) I_\lambda + \kappa_\lambda B_\lambda(T) + \beta_\lambda. \tag{2.6}$$

If we can neglect scattering, (2.6) further simplifies to

$$\frac{dI_\lambda}{\kappa_\lambda ds} = -I_\lambda + B_\lambda(T). \tag{2.7}$$

The form of (2.7) shows that the natural scale over which radiant intensity changes is a dimensionless quantity called the optical depth, τ_λ , defined so that

$$d\tau_\lambda \equiv \kappa_\lambda ds. \tag{2.8}$$

In the absence of emissions, the radiant intensity decays by a factor of $1/e$ over an optical depth of unity. The physical distance Δs over which this happens can be shown to be proportional to the mean free path of photons of wavelength λ . Thus optical depth, rather than actual distance, is the natural coordinate for radiative transfer. Using (2.8) we can write (2.7) in the form

$$\frac{dI_\lambda}{d\tau_\lambda} = -I_\lambda + B_\lambda(T). \tag{2.9}$$

We can make one more assumption that further simplifies matters. In a *plane-parallel atmosphere*, we assume that temperature and the concentration of absorbers are locally horizontally homogeneous, so that the variations in radiant intensity can be well approximated by vertical variations. In that case, since $ds = dz/\cos(\theta)$ (see Figure 2.2), we can write (2.7) as

$$\cos(\theta)\frac{dI_\lambda}{\kappa_\lambda dz} = -I_\lambda + B_\lambda(T), \tag{2.10}$$

where κ_λ and T are assumed to be functions of altitude (z) alone. In this case, it makes better sense to define the optical depth from

$$d\tau_\lambda \equiv \kappa_\lambda dz. \tag{2.11}$$

We will use this second definition and write the equation of radiative transfer for a plane-parallel atmosphere in the absence of scattering as

$$\cos(\theta)\frac{dI_\lambda}{d\tau_\lambda} = -I_\lambda + B_\lambda(T). \tag{2.12}$$

Defining $\mu \equiv \sec(\theta)$, we can write (2.12) as

$$\frac{d}{d\tau_\lambda}\left(I_\lambda e^{\mu\tau_\lambda}\right) = \mu B_\lambda e^{\mu\tau_\lambda}, \tag{2.13}$$

which can be integrated, starting from an optical depth of zero, to

$$I_\lambda = I_\lambda(0)e^{-\mu\tau_\lambda} + e^{-\mu\tau_\lambda}\int_0^{\tau_\lambda} \mu B_\lambda(T)e^{\mu\tau'}d\tau'. \tag{2.14}$$

Thus in a non-scattering, plane-parallel atmosphere, the monochromatic radiant intensity at any point is just that at the boundary, attenuated according to the optical depth times the secant of the zenith angle and added to by blackbody radiation from any emitters along the path, weighted by a function of the zenith angle, temperature, and the optical depth at that wavelength. To get the total radiant flux density through a horizontal plane at that wavelength, we would integrate the result using (2.1) and to get the flux over all wavelength we would use (2.2). The rate of radiative heating is just the vertical derivative of the flux.

One very important point about radiative transfer is that it is non-local. Perturbing the temperature or concentration of absorbers/emitters at any level in the atmosphere affects the amount of radiation passing through (and potentially partially absorbed by) every other level. In general, radiative heating cannot be modeled as a Fickian diffusion or Newtonian relaxation. The non-local character of radiation plays an important role in various tropical weather systems, as we will describe later in this chapter.

Apart from scattering, the physics clearly is wrapped up in the absorption coefficient, κ_λ, which also dictates what fraction of the blackbody radiation is emitted, according to Kirchoff's Law (2.4). These physics are too extensive and complex to review here in any comprehensive way, but broadly, most of the absorption in our atmosphere is owing to transitions in the quantized vibrational, rotational, and combined rotational-transitional states of molecules. These quantum transitions result in absorption/emission at particular wavelengths, but these absorption/emission lines are widened by Doppler broadening, owing to the random molecular motion relative to the radiation source, and pressure broadening due to collisional effects.

Molecular oxygen (O_2) and nitrogen (N_2) together comprise almost 99% of the mole fraction of the dry atmosphere, with argon (Ar) adding another 0.93%. Oxygen and nitrogen are simple homonuclear, diatomic molecules with no electric dipole moment and thus have very few degrees of freedom with which to interact with electromagnetic radiation. Likewise, argon has no interaction with radiation. Essentially all the absorption and emission in the atmosphere are owing to clouds, aerosols, and trace amounts of more complex molecules, notably water vapor

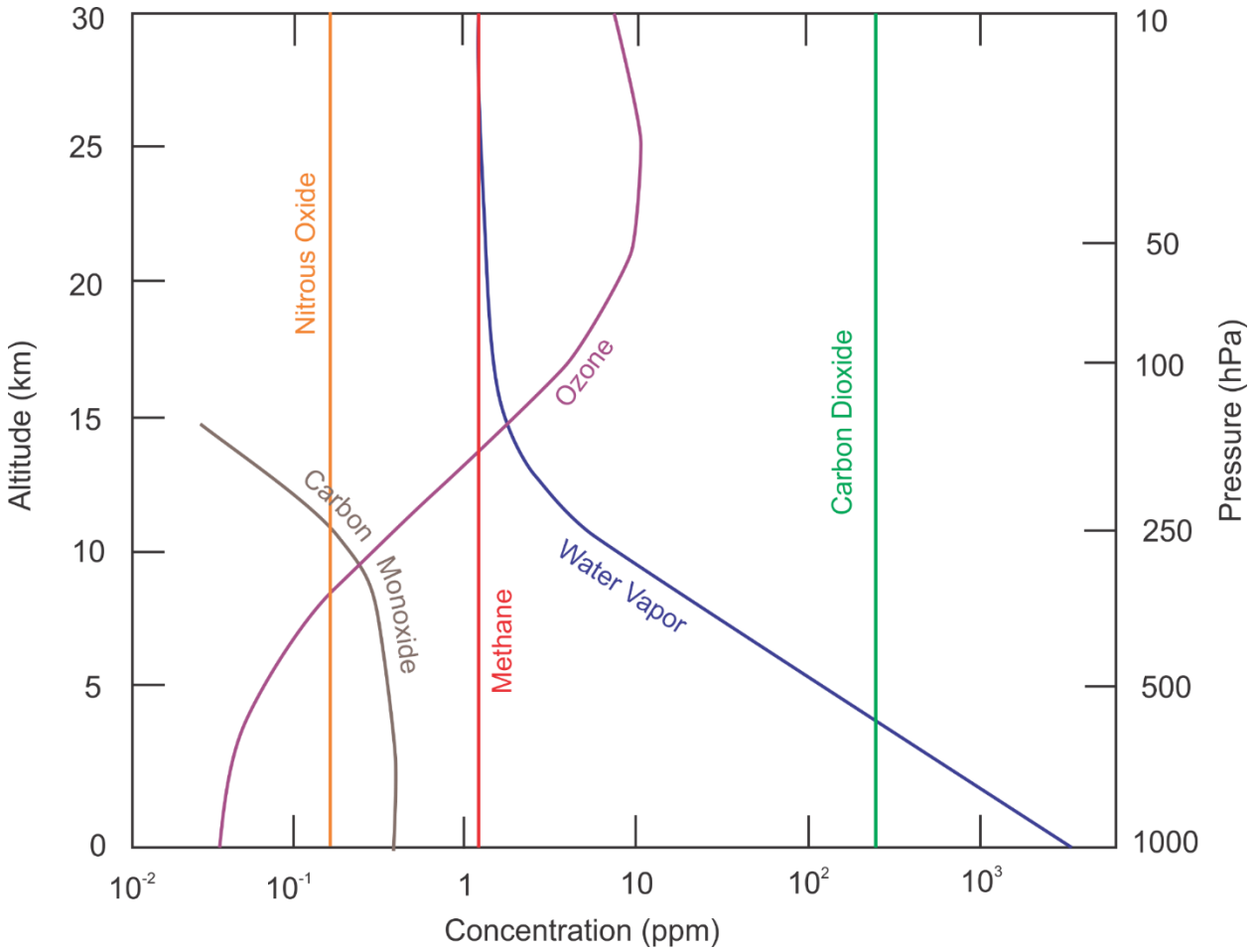

Figure 2.3: Mass concentrations (ppm) of some of the most important greenhouse gases in the atmosphere, as a function of altitude.

(H_2O), which is far and away the most abundant of these trace gases in the troposphere, but is highly variable in space and time, carbon dioxide (CO_2), methane (CH_4), ozone (O_3), carbon monoxide(CO), and nitrous oxide (N_2O). The time-mean, global-mean vertical distributions of these gases are shown in Figure 2.3, but note that the long-lived species (nitrous oxide, methane and carbon dioxide) are quite well homogenized in three-dimensional space and time. Ozone is formed in the middle and upper stratosphere by photodissociation of molecular oxygen by the high energy ultraviolet portion of the solar spectrum followed by recombination of some of the atomic oxygen with ordinary diatomic molecular oxygen, forming O_3. Ozone is unstable and itself breaks down into molecular and atomic oxygen by absorbing more ultraviolet radiation. These reactions absorb most of the ultraviolet portion of the solar spectrum, protecting life at the surface. Once formed, O_3 also absorbs and re-emits infrared radiation and is therefore a greenhouse gas.

Quantitatively, water vapor is the most important greenhouse gas owing to its relatively great abundance. Near the surface in the tropics, it can constitute up to 5% of the mole fraction of the atmosphere. Its variability and the variability of it condensed phase in the form of clouds, play a major role in tropical meteorology.

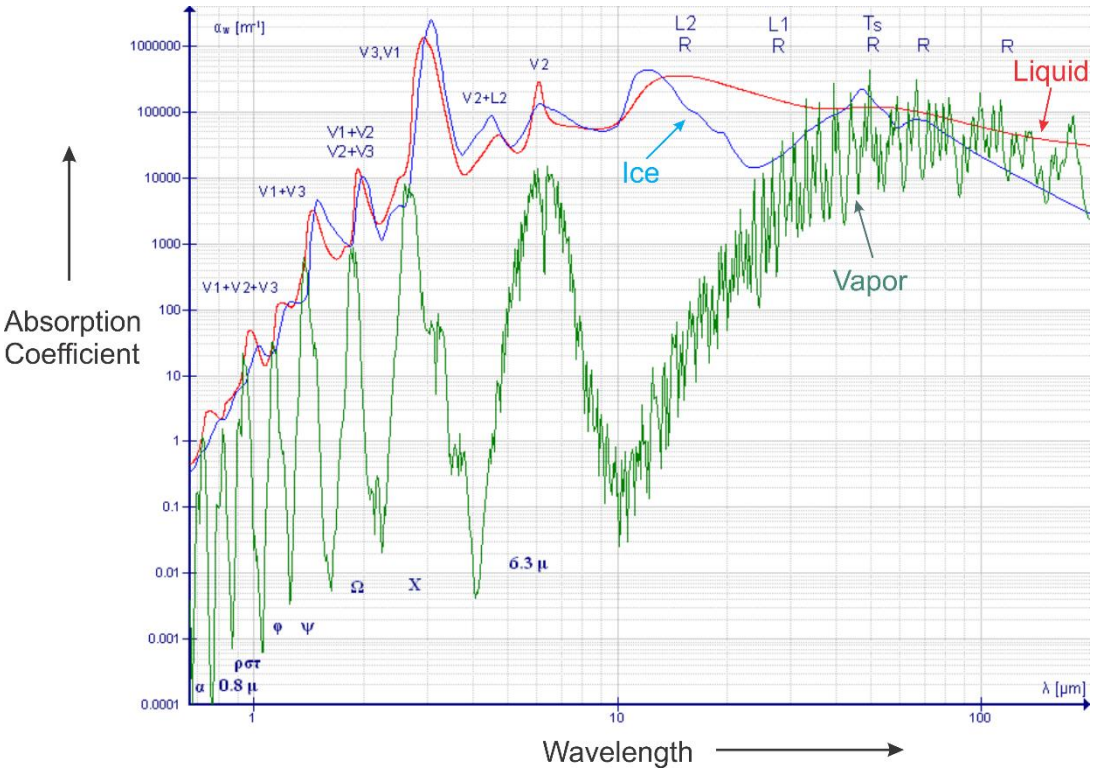

Figure 2.4 Absorption coefficient of water in its liquid (red), ice (blue), and vapor (green) phases in an important part of the terrestrial infrared spectrum, between $667\ nm$ *and* $200\ \mu m$*. Note that both axes are logarithmic.*

Next to water vapor, CO_2 is the most abundant greenhouse gas, and its very long residence time in the atmosphere ensures that it is well mixed. CO_2 and the other greenhouse gases play an important role in radiative transfer in the tropics and elsewhere, but unlike H_2O, their variability plays no important role in tropical weather and short-term climate variations.

Although the greenhouse gases constitute a very small fraction of the mass of the atmosphere, they collectively have a large effect on radiative transfer. An example of the complexity of atmospheric absorption is illustrated in Figure 2.4, which shows the absorption coefficient of water in all three of its phases, for wavelengths between $667\ nm$ and $200\ \mu m$. Pressure and Doppler broadening lead to an appreciable overlap in many of the absorption bands[2].

Let's examine some of the more prominent absorption/emission bands in our atmosphere. We begin by comparing the Planck (blackbody) curves of radiant flux density as a function of wavelength, for terrestrial and solar radiation, in the top panel of Figure 2.5. Because the effective emission temperatures of the two bodies are very different, there is hardly any overlap in their Planck functions and we can refer to solar and terrestrial radiation separately.(Note that

[2] The reader is encouraged to explore the myriad absorption/emission bands relevant to our atmosphere through David Archer's web-based program at http://climatemodels.uchicago.edu/modtran .

the solar intensity has been reduced by a very large factor to make it easier to compare the shape of the distributions.)

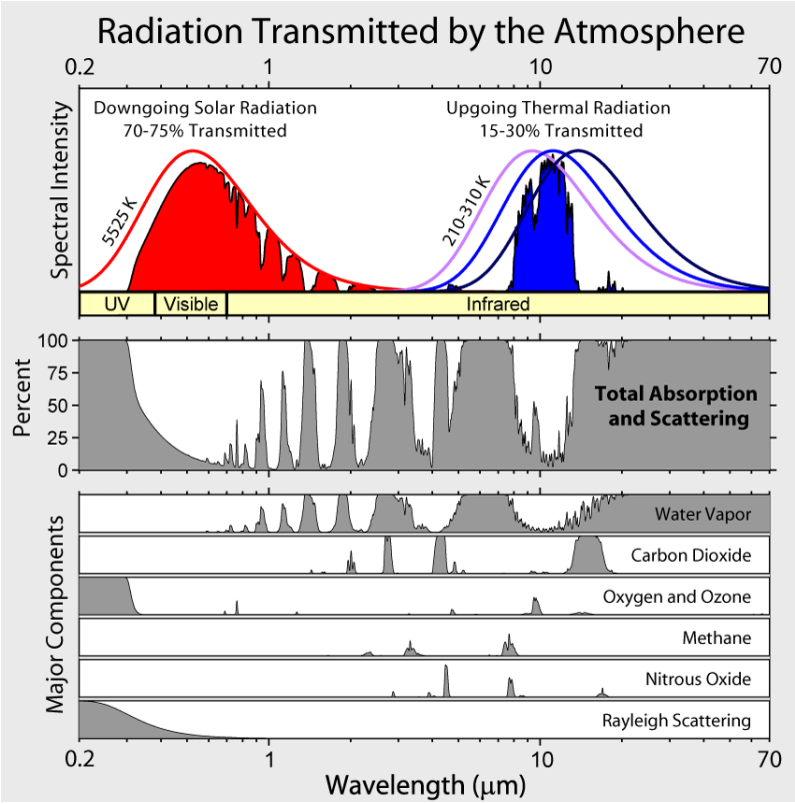

*Figure 2.5: Overview of absorption and scattering in the atmosphere. Top: Scaled blackbody curves for the sun (red) and the earth (black, blue, and magenta curves corresponding to different temperatures). The red and blue shaded areas represent the transmission of radiation. Middle: Fractional absorption and scattering of solar radiation passing downward toward the surface (left) and upward from the surface *right). Bottom panel: Breakdown of absorption among the greenhouse gases, and Rayleigh scattering by the gaseous constituents of the atmosphere.*

The color shading in the upper panels of Figure 2.5 shows how much radiant energy is actually transmitted through the cloud-free atmosphere at each wavelength. Most of the visible part of the solar spectrum is transmitted, which is presumably why our eyes evolved to detect light in this part of the spectrum. But at the infrared end of the solar spectrum, there is quite a bit of absorption, mostly by water vapor (see middle and bottom panels of Figure 2.5). Bear in mind that water vapor is highly variable in space and time. In the tropics, heating due to absorption of the infrared portion of the solar spectrum by water vapor can be quite large. Almost all the ultraviolet end of the spectrum is scattered and/or absorbed, the latter through the aforementioned photochemical reactions involved in ozone creation and destruction.

By contrast, much of the terrestrial spectrum is absorbed, with prominent absorption bands in water vapor (see Figure 2.4), carbon dioxide, methane, and nitrous oxide. There is a prominent window centered near $10\ \mu m$, which is at the peak of the blackbody curve corresponding to about 260 K.

The absorption spectra shown in Figure 2.5 do not include the effects of clouds. Clouds strongly absorb in the infrared and scatter solar radiation; the former acts to warm the surface while the

latter cools the surface. For a given infrared optical depth, high clouds are more effective at warming the surface than low clouds, because their effective emission temperature is lower.

2.2 Radiative equilibrium

Radiative equilibrium is achieved when each sample of the atmosphere, and the surface beneath it, emits as much radiation as it receives. Although the tropical troposphere is not near a state of radiative equilibrium, it is nevertheless of interest to calculate it since in a very loose sense, it is the state to which radiative processes are driving to drive the actual atmosphere. (This is only very roughly true because the presence of other processes, such as convection and large-scale circulation, changes the distributions of water vapor and clouds and so alter the radiative processes.)

Before undertaking a comprehensive calculation of radiative equilibrium characteristic of the tropical atmosphere, it is instructive to obtain a set of very approximate solutions that demonstrate some important, general features of the equilibrium state. Let's begin by making things as simple as possible. Beginning with the radiative transfer equation (2.14) in a non-scattering, plane-parallel atmosphere, we will consider a single isothermal layer of gas with temperature T at rest over a solid or liquid surface. We are going to make a radical (and obviously bad) approximation that the optical depth is independent of wavelength λ. This is called the *gray atmosphere* approximation. We will refer to this wavelength-independent optical depth as just τ_g, where the subscript "g" stands for "gray". Thus we can write (2.14) as

$$I_\lambda = I_\lambda(0)e^{-\mu\tau_g} + e^{-\mu\tau_g}\int_0^{\tau_g} \mu B_\lambda(T)e^{\mu\tau'}d\tau', \tag{2.15}$$

and since temperature is constant, we can take the blackbody function outside the integral and perform the integration, giving

$$I_\lambda = I_\lambda(0)e^{-\mu\tau_g} + B_\lambda(T)\left(1-e^{-\mu\tau_g}\right). \tag{2.16}$$

We next substitute this into (2.1), using $d\Omega = \sin(\theta)d\theta d\phi$, where ϕ is azimuth. Carrying out the integration in (2.1) then gives

$$F_\lambda = \left(1-\varepsilon\right)F_\lambda(0) + \varepsilon\pi B_\lambda(T), \tag{2.17}$$

where ε is an *emissivity*, given by

$$\varepsilon \equiv 1-e^{-\bar{\mu}\tau_g}, \tag{2.18}$$

where $\bar{\mu}$ is defined such that

$$e^{-\bar{\mu}\tau_g} \equiv 2\int_0^{\pi/2} \cos(\theta)\sin(\theta)e^{-\mu\tau_g}d\theta.$$

Finally, we can integrate (2.17) over all wavelengths to get the net flux per unit horizontal area, using Planck's Law (2.5) for the blackbody intensity:

$$F = \left(1-\varepsilon\right)F(0) + \varepsilon\sigma T^4, \tag{2.19}$$

where σ is the *Stefan-Boltzmann constant*, given to three significant figures by

$$\sigma = \frac{2\pi^5 k^4}{15c^2h^3} = 5.67 \times 10^{-8} Wm^{-2}K^{-4}. \tag{2.20}$$

Thus according to (2.19), the flux out one side of an isothermal, gray atmosphere is the incoming flux attenuated by $1-\varepsilon$ and added to by the ε multiplied by the wavelength-integrated blackbody radiation, which is proportional to the 4th power of the (absolute) temperature.

Now let's apply this to an isothermal atmosphere that is entirely transparent to solar radiation and completely opaque to infrared radiation $(\varepsilon = 1)$, overlying a surface whose shortwave and longwave emissivity is also unity (Figure 2.6).

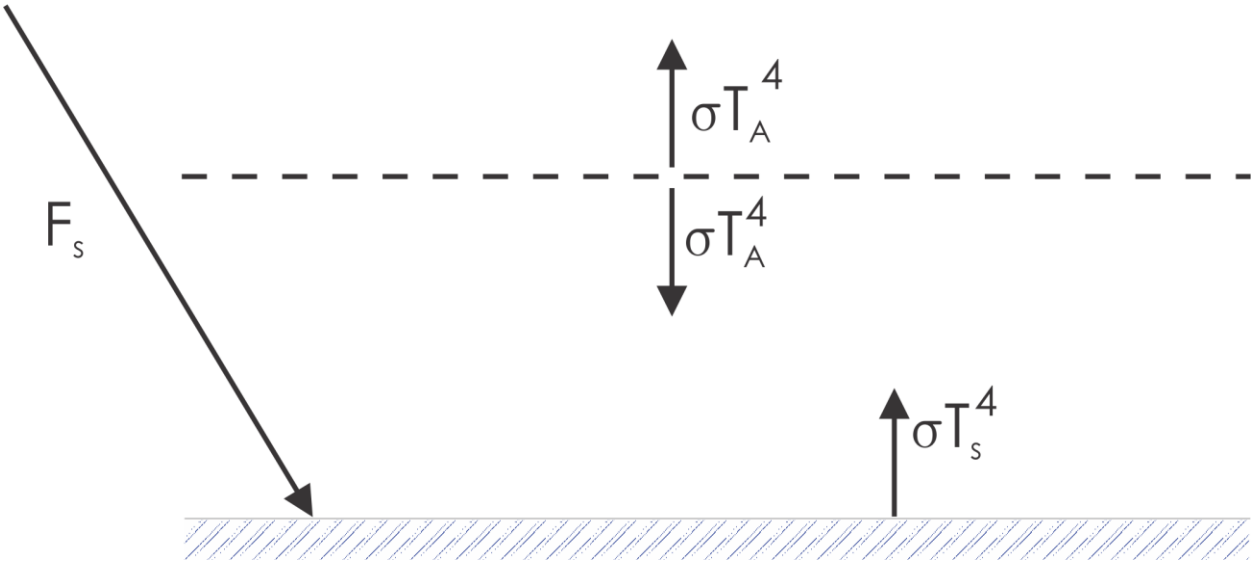

Figure 2.6: Plane-parallel, isothermal, non-scattering gray atmosphere transparent to incoming solar radiation, F_s, and opaque $(\varepsilon = 1)$ to infrared radiation. Atmospheric temperature is T_A and surface temperature is T_s.

First note that in the absence of an atmosphere, the total radiative flux from the surface would have to equal the incoming solar flux: $\sigma T_s^4 = F_s$. For global mean, annual mean insolation, after subtracting the portion reflected to space, this would yield a surface temperature of 255 K, which we will henceforth refer to as the *effective emission temperature* (T_e) of Earth. We can therefore represent the solar flux as σT_e^4. With the single opaque layer of isothermal gas shown in Figure 2.6, energy balance at the top of the atmosphere requires that $\sigma T_A^4 = F_s = \sigma T_e^4$, or $T_A = T_e$: The atmospheric temperature in this case is just the effective emission temperature of the planet. At the surface, however, energy balance requires that

$$\sigma T_s^4 = F_s + \sigma T_A^4 = 2\sigma T_e^4. \tag{2.21}$$

That is, the surface must be warm enough that its blackbody emission balances solar radiation *and* infrared back-radiation from the atmosphere. In this simple model, the surface receives the

same quantity of back-radiation from the atmosphere as it does directly from the sun. This back-radiation is conventionally called the *greenhouse effect* (though it has little to do with how an actual greenhouse works).

We next look very crudely at how temperature in an IR-opaque gray atmopshere varies with altitude. This can be illustrated by extending the single layer in Figure 2.6 to two layers, in Figure 2.7

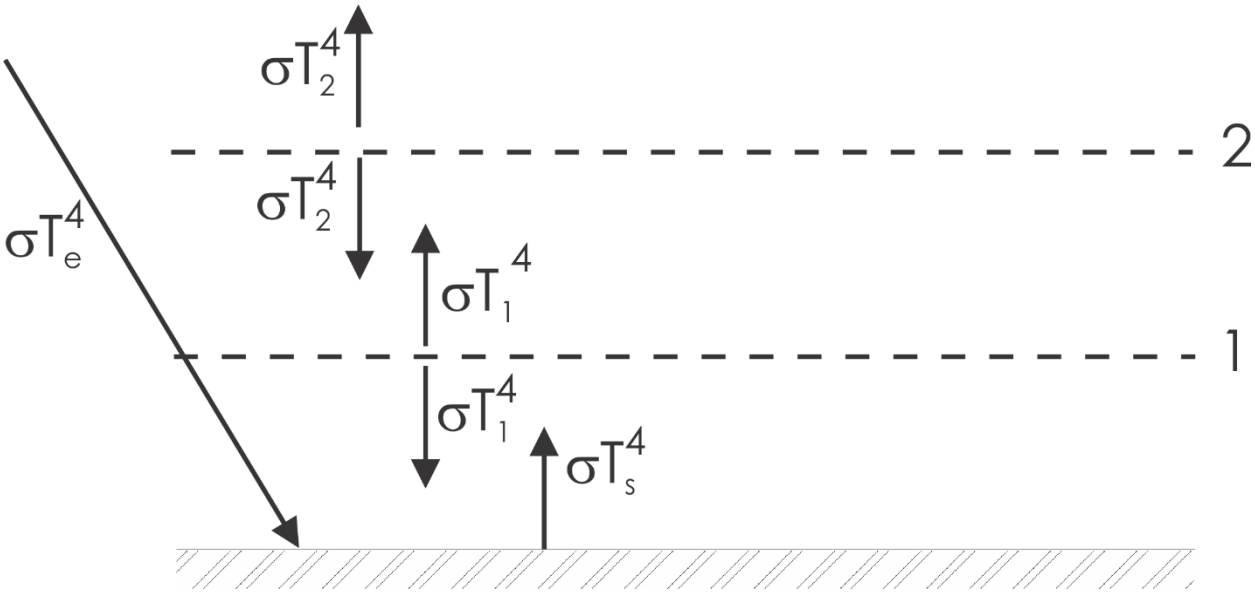

Figure 2.7: Extension of the one-layer model (Figure 2.6) to two layers. Incoming solar flux is expressed here as σT_e^4 .

As before, energy balance at the top requires that $T_2 = T_e$. Energy balance in the middle layer requires that

$$2\sigma T_1^4 = \sigma T_2^4 + \sigma T_s^4, \tag{2.22}$$

while the surface energy balance can be written

$$\sigma T_s^4 = \sigma T_1^4 + \sigma T_e^4. \tag{2.23}$$

Solving (2.22) and (2.23) yields

$$T_s = 3^{1/4} T_e, \quad T_1 = 2^{1/4} T_e. \tag{2.24}$$

It is straightforward to generalize this result to N layers (each one having an emissivity of unity), in which case the temperature of the n^{th} layer, counting down from the top, is just $n^{1/4} T_e$, and the surface temperature is $\left(N+1\right)^{1/4} T_e$. (Note here that adding opaque layers is somewhat like adding to the mass of greenhouse gases; it is not equivalent to dividing a fixed atmosphere into ever thinner layers, which would have progressively smaller emissivities.)

The top layer receives infrared radiation from the layer below it, but nothing from above, whereas the bottom layer receives radiation from both the surface the top layer, so it is hardly surprising that its temperature is higher than that of the top layer. In general, *in radiative equilibrium in a gray atmosphere with uniform emissivity, temperature decreases with altitude*.

In this problem, the radiative transfer is effectively "local" in the sense that each layer only influences its neighbor, because each layer absorbs all the radiation incident upon it. But if we relax the assumption of unitary emissivities, then some radiation from each payer will penetrate through to be partially absorbed by all other layers. This makes the problem algebraically more complex.

We look at two more cases in which we add two layers of very *low* emissivity, as illustrated in Figure 2.8.

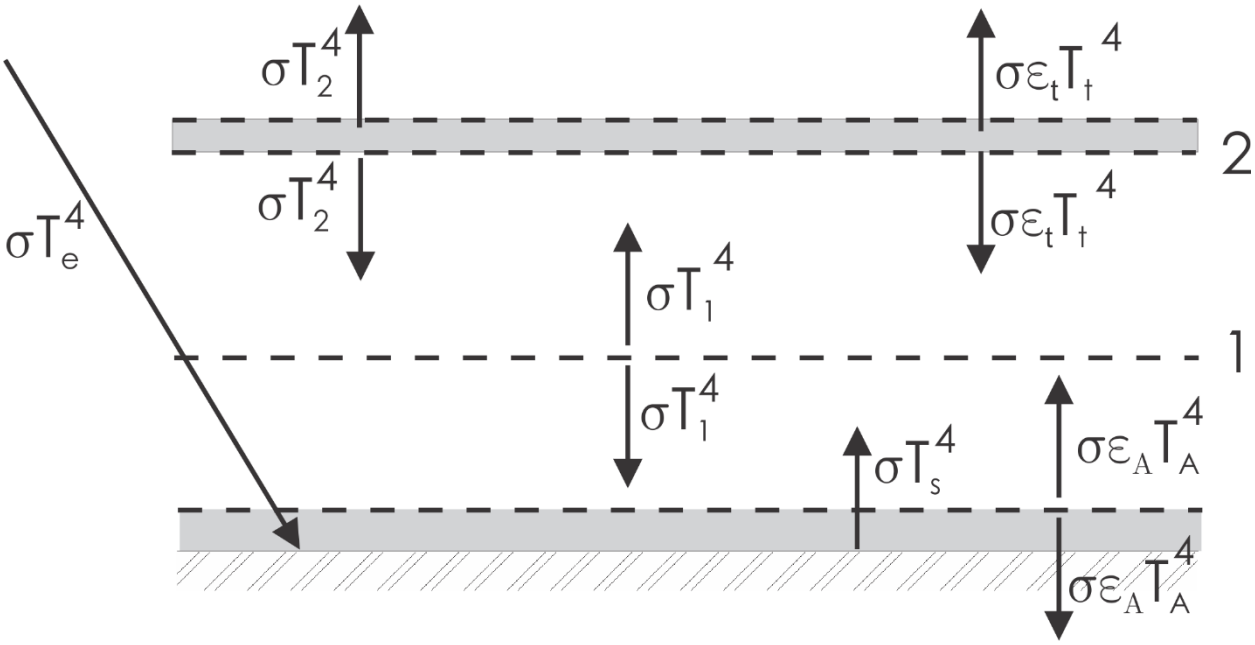

Figure 2.8: Two-layer model as in Figure 2.7, but with two additional layers of vanishingly small emissivities: one at the top, and once adjacent to the surface.

The infrared emissivities of the new top and bottom layers are ε_t and ε_A,respectively. If we consider the limit in which they vanish, then these new layers will have no effect on the temperature of the main layers and the surface, given by (2.24) (together with $T_2 = T_e$). On the other hand, the energy balance of the top layer requires that

$$2\varepsilon_t \sigma T_t^4 = \varepsilon_t \sigma T_2^4, \tag{2.25}$$

that is, the energy emitted up and down from this new layer must balance the partial absorption by this layer of energy upwelling from the second main layer. Thus $T_t = 2^{-1/4} T_e$. Therefore, *parts of an atmosphere in radiative equilibrium can have temperatures less that the effective emission temperature.* (In fact, this is usually the case.)

Likewise, for the thin layer next to the surface, the energy balance is

$$2\varepsilon_A \sigma T_A^4 = \varepsilon_A \sigma T_1^4 + \varepsilon_A \sigma T_s^4, \tag{2.26}$$

or $T_A^4 = \frac{1}{2}\left(T_s^4 + T_1^4\right)$. The thin layer of air in contact with the surface has a temperature intermediate between that of the surface and that of the first main layer of gas. The essential point here, and one that is important for understanding a variety of tropical weather phenomena, including tropical cyclones, is that in radiative equilibrium, *a discontinuity in emissivity (as between a gas and a solid or liquid surface) entails a discontinuity in temperature*. Thus, *for a gas overlying a surface, radiative equilibrium implies thermodynamic disequilibrium*. We will return to this important point time and again, but for now note that for a variety of physical and biological systems, thermodynamic disequilibrium is the basis for the development of self-organizing structures, even in otherwise chaotic background states (Nicolis and Prigogine, 1977).

We can obtain analytic radiative equilibrium solutions for a non-scattering, plane-parallel gray atmosphere that are continuous in the vertical for some special cases. We begin by re-writing (2.12) for a gray atmosphere that is transparent to solar radiation as

$$\cos(\theta)\frac{dI_\lambda}{d\tau_g} = -I_\lambda + B_\lambda(T). \tag{2.27}$$

Because τ_g is independent of wavelength, we substitute (2.27) into (2.1) and (2.2) and integrate over solid angle in a single hemisphere, and wavelength to obtain

$$\overline{\cos(\theta)}\frac{\partial F}{\partial \tau_g} = -F + \sigma T^4, \tag{2.28}$$

where $\overline{\cos(\theta)}$ is a suitably defined mean cosine of the zenith angle. In deriving (2.28) we have not specified whether the flux is upward or downward, and it helpful to divide the flux at each level into upward and downward traveling components:

$$F = U - D. \tag{2.29}$$

Defining $\tau_v \equiv \tau_g / \overline{\cos(\theta)}$, we write separate equations for the up and down components:

$$\frac{\partial U}{\partial \tau_v} = -U + \sigma T^4, \tag{2.30}$$

and

$$-\frac{\partial D}{\partial \tau_v} = -D + \sigma T^4. \tag{2.31}$$

Radiative equilibrium requires that there be no convergence of the net flux, $U - D$, through each level. Thus adding (2.30) to (2.31) gives

$$\frac{\partial}{\partial \tau_\nu}(U-D)=0=-U-D+2\sigma T^4, \tag{2.32}$$

while subtracting (2.31) from (2.30) yields

$$\frac{\partial}{\partial \tau_\nu}(U+D)=-U+D. \tag{2.33}$$

From (2.32) the net flux, $U-D$ must be independent of optical depth, and at the top of the atmosphere $D=0$ and the upward flux, U_∞, must equal the net absorbed solar flux (after subtracting the fraction reflected), S, so $U-D=S$. The solutions to (2.33) that meet the boundary conditions at the top of the atmosphere, $U_\infty=S, D_\infty=0$, are then

$$\sigma T^4=\frac{S}{2}(1+\tau_{\nu\infty}-\tau_\nu), \tag{2.34}$$

$$D=\frac{S}{2}(\tau_{\nu\infty}-\tau_\nu), \tag{2.35}$$

and

$$U=S\left[1+\frac{1}{2}(\tau_{\nu\infty}-\tau_\nu)\right]. \tag{2.36}$$

Here $\tau_{\nu\infty}$ is the infrared optical depth of the whole atmosphere. Note that as τ_ν approaches $\tau_{\nu\infty}$ at the top of the atmosphere, $\sigma T^4 \to \frac{S}{2}$, which is the same solution (2.25) we found for the layer of small emissivity at the top of the layer model.

Note also that the downward infrared flux at $\tau_\nu=0$ is $S\tau_{\nu\infty}/2$. So for optically thin atmospheres, there is hardly any downwelling infrared flux at the surface, while the flux can exceed the solar flux for optically thick atmospheres. If we insert, at z=0, a rigid or liquid surface of unitary emissivity, then the energy balance at the surface is

$$\sigma T_s^4=S+D(0)=S\left(1+\frac{\tau_{\nu\infty}}{2}\right). \tag{2.37}$$

Comparing to the air temperature at $\tau_\nu=0$, from (2.34), we see that the difference between the surface and air temperatures is given by

$$\sigma\left(T_s^4-T^4(0)\right)=\frac{S}{2}. \tag{2.38}$$

Curiously, the difference in the fourth powers of the air and ground temperatures is one-half the incoming solar flux, regardless of infrared opacity. If we let $T(0) = T_s - \Delta T$ and expand $T^4(0)$ to order one in ΔT, assuming that $\Delta T / T_s << 1$, then it is approximately true that

$$T_s - T(0) \simeq \frac{S}{8\sigma T_s^3}, \tag{2.39}$$

So the ground-air temperature difference in radiative equilibrium drops off rapidly with surface temperature (and thus with infrared opacity).

We can plot these solutions as a function of altitude or pressure, given a particular distribution of optical depth with altitude. Suppose, for example, that optical depth from the surface upwards increases linearly with the difference between actual and surface pressures, according to

$$\tau_v = \tau_{v\infty}\left(\frac{p_0 - p}{p_0}\right), \tag{2.40}$$

where p_0 is the surface pressure. The solutions (2.34) and (2.39) are plotted in Figure 2.9 for particular choices of $\tau_{v\infty}$ and p_0. Note that the plot is logarithmic in pressure, which is approximately linear in altitude in a hydrostatic atmosphere.

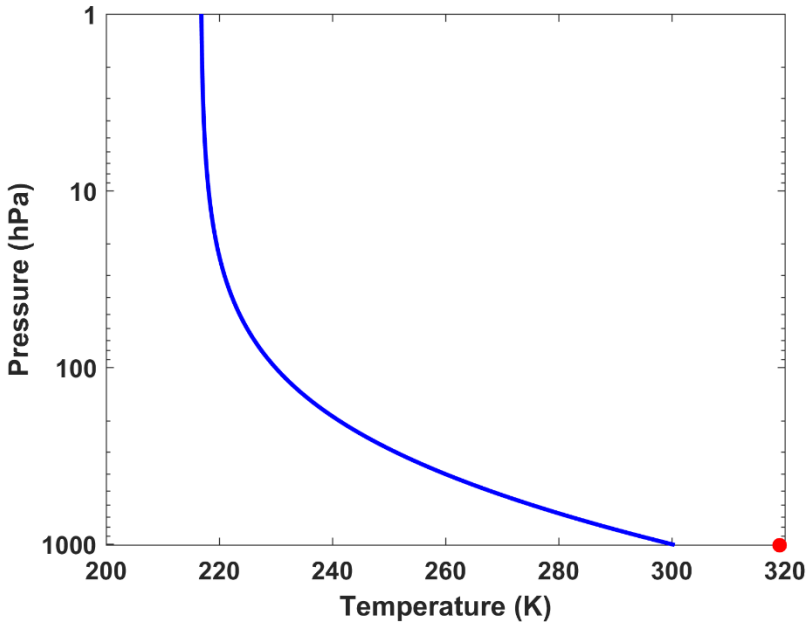

Figure 2.9: Radiative equilibrium temperature of a non-scattering, plane-parallel, gray atmosphere that does not absorb solar radiation, as given by (2.34) and (2.39) when the optical depth varies with pressure according to (2.40) with $S = 250\ Wm^{-2}$, $\tau_{v\infty} = 2.7$, *and* $p_0 = 1010\ hPa$. *The red dot shows the solution for the surface temperature.*

As with the discrete layer models, temperature decreases with altitude, but since the infrared optical thickness becomes small in the upper atmosphere, the temperature becomes nearly isothermal. As we shall see presently, the actual temperature of the tropical atmosphere

increases in the stratosphere (above the level where the pressure is approximately 100 hPa), and this is due to absorption of high energy ultraviolet solar radiation in the middle and upper stratosphere. As noted previously, radiative equilibrium entails a profound thermodynamic disequilibrium between the surface and the atmosphere just above it, a fact of great consequence for tropical meteorology and climate.

While the approximation of a gray atmosphere is very helpful in revealing some of the most essential aspects of radiative transfer and radiative equilibrium, it is quantitatively a poor approximation to the real atmosphere, with its very complex set of absorption/emission lines. Fortunately, the spectra for all the important greenhouse gases in the atmosphere have been calculated for a range of temperatures and pressures and are included in a comprehensive database known as HITRAN (*hi*gh-resolution *tran*smission molecular absorption database; see www.hitran.org). But a comprehensive, line-by-line treatment of radiative transfer is too expensive to use in most atmospheric models and so we turn to band-averaged codes which are much faster and which have been carefully compared to both observations and HITRAN data.

One such band-averaged radiation code is included as part of the online supplement to this book. This is coupled to a comprehensive representation of convection (about which more in due course), but for now we turn off the convection and look at the radiative equilibrium solution representative of the tropical atmosphere. This is problematic, because moist convection lofts water from its source at the surface into the free atmosphere; without it, there is no control on atmospheric water vapor, the most important greenhouse gas. Removing water vapor altogether would result in very low temperatures, but retaining values characteristic of the tropical atmosphere results in strong supersaturations in a pure radiative equilibrium calculation. We here choose the intermediate route of holding the relative humidity (the ration of the vapor pressure to its saturation value) to be a fixed function of altitude, characteristic of the tropical atmosphere.

Figure 2.10 shows a calculation of pure radiative equilibrium using observed constant concentrations of carbon dioxide, methane, and nitrous oxide, CFC11, and CFC12, a fixed profile of ozone representing a global average, and water vapor calculated from the model predicted temperature and a fixed vertical profile of water vapor characteristic of the tropical atmosphere. This calculation does not include the effect of clouds on radiative transfer and uses instead a representative fixed albedo of 0.25 and a fixed, annual mean insolation at 23 degrees north latitude. The lower boundary is a thin slab of water whose temperature is also calculated from radiant energy balance; the equilibrium water temperature is shown by the red dot in Figure 2.10. The dashed blue line in Figure 2.10 represents the mean temperature profile over more than 800 balloon soundings from the equatorial North Pacific island of Kapingamorangi, taken as part of the TOGA COARE field campaign.

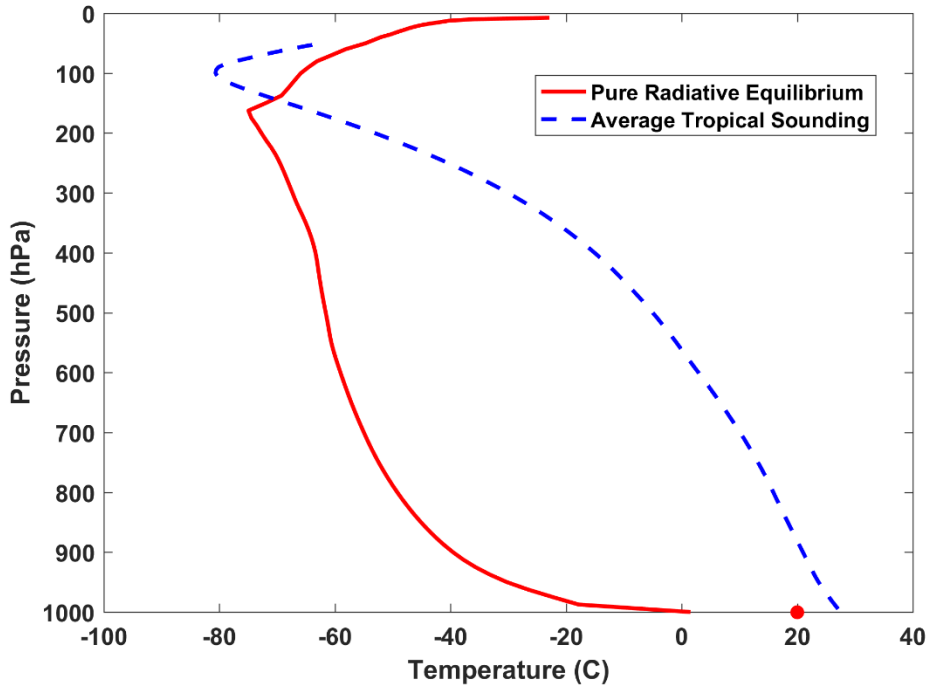

Figure 2.10: Calculation of pure radiative equilibrium (red curve) for the tropical atmosphere, under the assumption that the relative humidity is fixed at a representative tropical profile. The calculated temperature of the underlying water slab is shown by the red dot. (See text for further details.) The dashed blue line represents the average of over 800 rawinsonde temperature profiles from the equatorial North Pacific island of Kapingamarangi.

The radiative equilibrium shares some features with the highly idealized analytic solution shown in Figure 2.9. Both have a temperature jump of around 20 K between the surface and the atmosphere just above it, and both show a rapid decay of temperature with altitude, tapering off toward a constant temperature higher up. But the band-averaged solution then shows some notable departures. Above 400 hPa, the temperature lapse rate increases again, reaching a sharp minimum at around 175 hPa. This is likely owing to a layer of relative high humidity in the upper troposphere which, in the moist convective atmosphere results from outflow from deep convective clouds. According to (2.34), if the infrared optical depth increases more rapidly, because of a layer of higher concentration of absorbers, the temperature should decrease more rapidly. In stark contrast to the simply solution, temperature increases rapidly above this tropopause, and this is owing to absorption of solar radiation by ozone in the stratosphere, which was neglected in the simple gray model.

The radiative equilibrium solution shown in Figure 2.10 bears little resemblance to the temperature profiles seen in the real tropical atmosphere (dashed blue curve in Figure 2.10). The whole troposphere is substantially colder than reality, and the curvature of the temperature profile is mostly opposite to that seen in the real soundings. The relatively low surface temperature and the steep decline of temperature with altitude imply, though the Clausius-Clapeyron equation coupled with our assumption of fixed relative humidity, that the water vapor concentration is much lower than in the real atmosphere. Since this is the most important greenhouse gas, the whole system is much colder than observed.

Why is the radiative equilibrium solution such a poor representation of the tropical atmosphere? Far and away the most important reason for this is that the radiative equilibrium solution is strongly unstable to convection, which is as important as radiation in transferring energy through the tropical atmosphere and which also serves to loft the most important greenhouse substance – water, in all three of its phases. Thus we turn to the important subject of convection.

2.3 Dry convection

A dynamical system in equilibrium is unstable if there are any small disturbances, added to the equilibrium state, that amplify with time. An unstable system will generally evolve to a state, which may be time-dependent, that differs from the original equilibrium. By contrast, small perturbations added to a stable equilibrium will either oscillate about that equilibrium or decay (or both), leaving the original equilibrium state essentially unaltered. A meta-stable equilibrium is stable to infinitesimal perturbations but unstable to a sufficiently large disturbance.

A simple system that can exhibit each of these stability states is a frictionless marble on a wavy surface in a constant gravitational field. The marble sitting at the bottom of a depression, when displaced in any direction, will roll back towards the bottom and will oscillate around the lowest point. Naturally, this equilibrium is stable. A marble on a perfectly flat portion of the surface is neutrally stable; when displaced it will not accelerate in any direction. When the marble is balanced on the top of a hill, it is in equilibrium, but any displacement will cause it to accelerate toward a depression, so that equilibrium is unstable. Now imagine a marble at rest on a saddle point: The topography goes uphill in, say, the positive and negative x direction, but downhill in the positive or negative y direction. (Think of the shape of a horse saddle.) If displaced exactly in the x direction, it will accelerate back toward the saddle point, but in any other direction it will not return to its original position. This is also an unstable equilibrium because there is at least one perturbation that amplifies. Finally, think of a hill with a small depression at its top. A marble in the base of that depression is stable because if pushed very slightly in any direction it will accelerate back towards it initial state. On the other hand, if pushed hard enough, it will roll over the top of the rim and accelerate away from the hill. This equilibrium state is metastable.

In thinking about the marble, you probably made some tacit assumptions about the system without necessarily being conscious of them. You almost certainly assumed that the mass of the marble is invariant….it did not accrete or lose mass on the way. You probably also assumed that after the initial displacement, the sum of the marble's kinetic and potential energies is conserved; there are no demons around giving the marble a shove. Most stability problems assume the dynamical system has certain invariants, like mass and total energy.

Now consider a horizontally homogeneous gas in hydrostatic equilibrium at rest over a rigid or solid surface, also in a state of radiative equilibrium. How can we tell if this system is stable?

As with the marble on a wavy surface, we will test the system for stability by vertically displacing a sample adiabatically and reversibly, so that it conserves its entropy. If the sample displaced upward obtains positive buoyancy, it will accelerate upward and thus the state is unstable. (Likewise, if the parcel is displaced downward and obtains a negative buoyancy, the system is unstable.) The equations of motion can be used to show that buoyancy is proportional to the perturbation of specific volume (inverse density) along a surface of constant pressure.

Thus, if the specific volume of a sample of air displaced upward is larger than that of its environment at the same pressure level, it will accelerate upward, in the same direction as the

original displacement, and the state will be unstable. But in a gas, specific volume is not conserved and so this is not a simple matter of that sample taking its original specific volume with it. So we have to identify an adiabatic invariant of the air that we can use to deduce the specific volume. Here we use the specific entropy, s, of the sample as a quantity conserved under reversible adiabatic displacements from which one can deduce specific volume.

To relate specific volume to entropy we use one of many Maxwell relations from the field of thermodynamics. Not all students are familiar with these, so we will derive the relevant relation here. We begin with a statement of the first law of thermodynamics:

$$dk = Tds - \alpha dp, \tag{2.41}$$

where k is the specific enthalpy, T is temperature, s is specific entropy, α is specific volume, and p is pressure. From (2.41) it is evident that

$$\left(\frac{\partial k}{\partial s}\right)_p = T, \tag{2.42}$$

and

$$\left(\frac{\partial k}{\partial p}\right)_s = \alpha, \tag{2.43}$$

where the subscripts on the partial derivatives denote quantities being held constant. Now in partial differentiation, the order of differentiation is immaterial, so

$$\left(\frac{\partial}{\partial s}\right)_p \left(\frac{\partial k}{\partial p}\right)_s = \left(\frac{\partial}{\partial p}\right)_s \left(\frac{\partial k}{\partial s}\right)_p. \tag{2.44}$$

Using (2.42) and (2.43) in (2.44) gives

$$\left(\frac{\partial \alpha}{\partial s}\right)_p = \left(\frac{\partial T}{\partial p}\right)_s. \tag{2.45}$$

This is the desired Maxwell relation and we will make extensive use of it through the rest of this book. It is valid for a homogeneous gas, in which any state variable can be written as a function of any other two state variables. So, using the chain law, we can write

$$d\alpha = \left(\frac{\partial \alpha}{\partial s}\right)_p ds + \left(\frac{\partial \alpha}{\partial p}\right)_s dp. \tag{2.46}$$

Since buoyancy is proportional to perturbations of specific volume at constant pressure, we can use (2.45) and (2.46) to write an expression for perturbations of specific volume at constant pressure:

$$\alpha' = \left(\frac{\partial T}{\partial p}\right)_s s', \tag{2.47}$$

where the primes denote perturbation of the sample's properties from those of its environment. Finally, buoyancy itself is just the specific volume perturbation multiplied by the acceleration of gravity and divided by the mean state specific volume:

$$B = g\frac{\alpha'}{\bar{\alpha}} = \frac{g}{\bar{\alpha}}\left(\frac{\partial T}{\partial p}\right)_s s', \tag{2.48}$$

where g is the acceleration of gravity. Since the mean state is in hydrostatic balance, it is more compact to write (2.48) as

$$B = \Gamma_d s', \tag{2.49}$$

where Γ_d is the dry adiabatic lapse rate, defined

$$\Gamma_d \equiv -\left(\frac{\partial T}{\partial z}\right)_s. \tag{2.50}$$

It is a simple exercise to derive from the first law of thermodynamics that, for a homogeneous gas, $\Gamma_d = g / c_p$, where c_p is the heat capacity at constant pressure. In our atmosphere, the dry adiabatic lapse rate Γ_d, is nearly $1\,K/100\,m$.

The relationship between buoyancy and entropy, given by (2.49), is extraordinarily simple and powerful. A homogeneous atmosphere in hydrostatic balance will be unstable if its entropy decreases with altitude. Under these circumstances, a sample displaced upward reversibly and adiabatically will carry its entropy with it, and since the environmental entropy decreases upward, it will have an entropy larger than that of its environment and accelerate upward, in the same direction as the original displacement. Conversely, a gas at rest with entropy increasing upward is stable and therefore supports oscillations, which in meteorology are referred to as internal gravity waves.

Figure 2.11 shows the vertical distribution of the specific entropy of the radiative equilibrium temperature profile shown in Figure 2.10. From the first law of thermodynamics, the entropy may be expressed

$$s_d = c_p \ln(T / T_0) - R_d \ln(p / p_0), \tag{2.51}$$

where T_0 is an arbitrary reference temperature and p_0 is an arbitrary reference pressure. (Note that entropy is arbitrary to within an additive constant; in calculating entropy here we have normalized temperature and pressure by representative values, and one effect of this is to make the entropy negative at certain altitudes.) We have added the subscript *d* to the entropy here to denote the entropy of dry air. Also shown by the red dot in Figure 2.11 is the specific entropy of air at the same temperature as the underlying layer of liquid water.

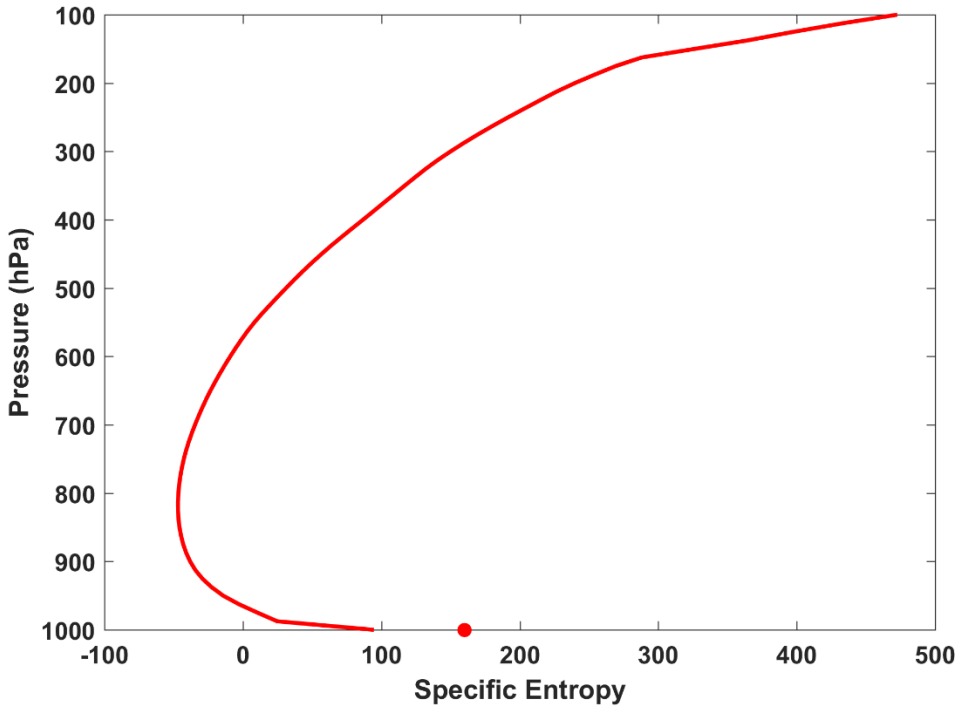

Figure 2.11: Vertical distribution of specific entropy corresponding to the radiative equilibrium temperature profile shown in Figure 2.10. The specific entropy of air in thermodynamic equilibrium with the underlying surface is shown by the red dot. Note that the value of the specific entropy is arbitrary to within an additive constant.

The profile is clearly unstable. A sample of air lifted upward from the surface will have a positive entropy perturbation up to about 400 hPa, while a sample that has been brought to the temperature of the underlying water (red dot) will be buoyant all the way up to about 300 hPa. Thus we would expect virtually the whole troposphere, starting from a state of radiative equilibrium, to convect.

What form does the convection take, and what is the nature of the new equilibrium it establishes? In our atmosphere, the effective Reynolds Number of convective flows is extremely large, so that convection is always fully turbulent – molecular diffusion plays no direct role.

As one might expect, turbulent convection consists of a spectrum of turbulent eddies with a strong correlation between vertical velocity and specific volume, so that that enthalpy is turbulently transported upward, heating the fluid aloft and cooling it at lower levels.

In chaotic systems such as convection, we usually have to give up on deterministic models of individual convective elements and turn instead to statistical descriptions of the flows. These are often the most useful descriptions for the purpose of representing the ensemble effects of the turbulence on larger scales of motion that we do wish to predict more deterministically.

Among the first questions we might raise about the nature of dry convective turbulence, is what determines characteristic scales for vertical velocity, plume radius, and buoyancy? How does the ensemble- or time-average temperature vary with altitude? How does the convection affect the temperature jump between the lower boundary and the atmosphere just above it? In confronting highly complex fluid flows to obtain answers to even simple questions such as

these, it is often useful to contemplate systems with an extremely limited set of control parameters. If they are sufficiently limited, then inferences can be made on strictly dimensional grounds, and tested against observations or laboratory experiments.

A classic example of dimensional reasoning is the case of homogeneous, isotropic three-dimensional turbulence in an infinite incompressible fluid. Kinetic energy is injected at large scales and cascades downscale ultimately to such small scales that it is dissipated by molecular diffusion. The critical hypothesis here is that above these smallest scales, molecular diffusion plays no significant role, and the only external parameter that matters is the rate of kinetic energy injection per unit mass. We must also assume that we are examining scales small enough that they are not directly affected by the large scale at which energy is presumed to be injected.

This injection rate, call it I, has the dimensions of kinetic energy per unit time per unit mass, or L^2t^{-3}, where L represents length and t represents time. Suppose we ask how the spectral density of kinetic energy per unit mass, E_k, depends on wavenumber. That quantity has dimensions L^3t^{-2}. If E_k depends only on I, then dimensionally there is only one choice: $E_k \sim I^{2/3}k^{-5/3}$, where k is the wavenumber. Thus the spectral kinetic energy density per unit mass must fall off as the 5/3 power of the wavenumber. The dimensionless constant of proportionality must be determined by experiment.

This hypothesis, by the Russian mathematician Andrei Kolmogorov in 1941, has been tested experimentally in high Reynolds Number homogeneous flows in statistical equilibrium and found to be very well verified.

If we consider scales so small that molecular viscosity, ν (dimensions L^2t^{-1}), plays a role, then we can form a length scale, l, from I and ν: $\nu^{3/4}I^{-1/4}$. This is called the *Kolomogorov length* and can be interpreted as an upper bound on the length scale of eddies influenced directly by molecular viscosity. Scales larger than this, but smaller than the scales at which energy is injected, are referred to as the inertial subrange and are the scales to which the Kolomogorov scaling applies.

It is possible to formulate an equally simple problem for convection[3]. The setup is illustrated in Figure 2.12.

[3] This formulation has been attributed to the German fluid dynamicist Ludwig Prandtl.

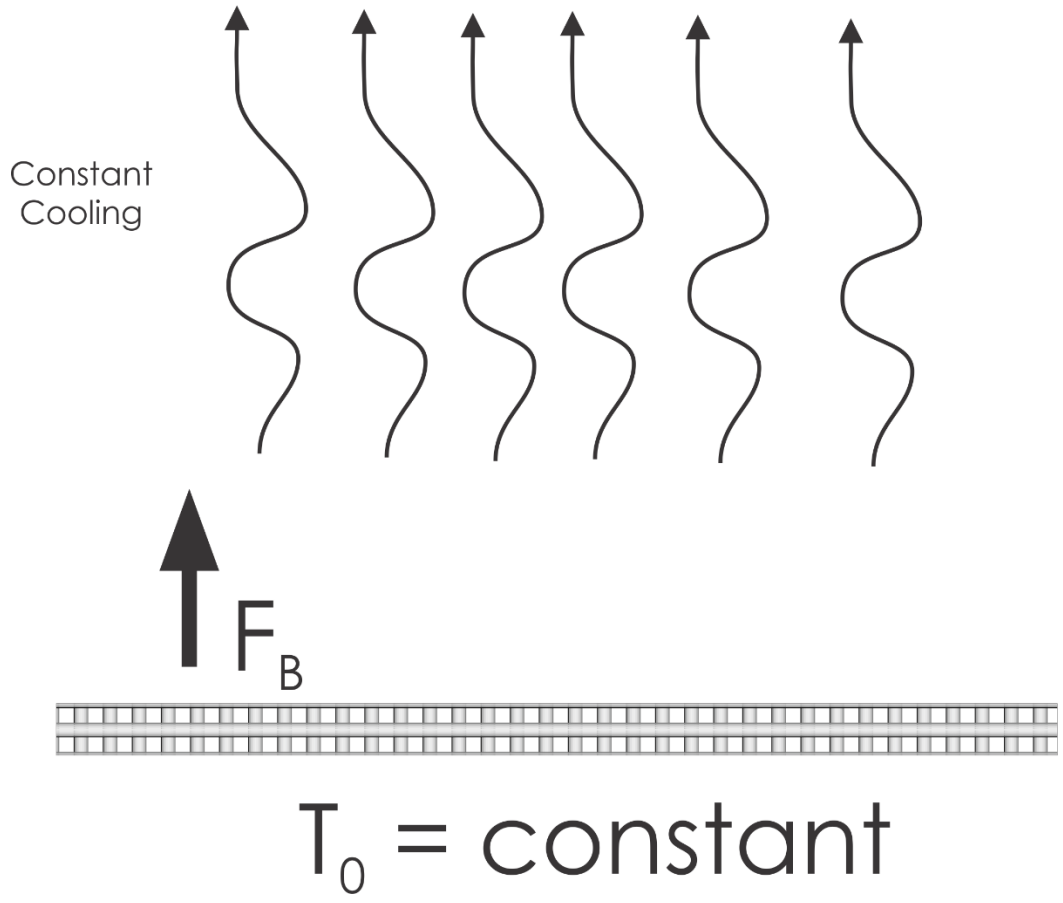

Figure 2.12: Semi-infinite, Boussinesq fluid subject to a constant rate of cooling, overlying a rigid plate held at fixed temperature T_0.

Imagine a semi-infinite, Boussinesq fluid in a constant gravitational field and cooled at some constant rate per unit mass, overlying a rigid plate at fixed temperature, T_0. A Boussinesq fluid is one that is nearly incompressible, so that density fluctuations only matter in the buoyancy term of the equations of motion. Otherwise, the fluid may be considered incompressible and, in particular, obeys the incompressible version of the mass continuity equation.

The fluid initially cools owing to the imposed cooling, but is heated from below by contact with the surface. This heating destabilizes the fluid and produces convection. After a very long time, the convergence of the upward flux of heat by the presumably turbulent convection comes into statistical equilibrium with the imposed cooling, and the system reaches a statistical equilibrium state. For overall energy balance, the heat flux F through the lower boundary must equal the vertically integrated imposed cooling rate, $\dot{Q}$:

$$F = \int_0^\infty \dot{Q} dz. \tag{2.52}$$

The surface heating produces temperature fluctuations, but according to the Boussinesq approximation, these only influence the system through the buoyancy. Thus the important external parameters is not the heat flux but the buoyancy flux:

$$F_B = g\beta F / c_p, \tag{2.53}$$

where β is the coefficient of thermal expansion of the fluid. Note from (2.54) that the imposed cooling per unit mass is infinitesimal, such that its integral through the infinite depth of the fluid is a finite constant. We might imagine that very close to the surface, the turbulent convective eddies are small, with their length scale constrained by their distance from the surface. We will assume that the boundary is thermally rough, with a typical thermal roughness scale z_0^T, a scale we will consider to be large compared to the scales at which molecular diffusion is important.

Above the roughness scale z_0^T, we shall assume, in analogy to Kolomorogov's hypothesis, that molecular diffusion plays no direct role. If that is the case, then the imposed cooling, as translated to the surface buoyancy flux per unit area (dimensions L^2t^{-3}), given by (2.53) is the only control parameter in the problem. If that is indeed the case, we can make several deductions on purely dimensional grounds:

1. The characteristic size of the turbulent eddies scales with the altitude z above the surface.
2. The characteristic buoyancy of the eddies, $g\beta|T'|$, scales as $F_B^{2/3}z^{-1/3}$.
3. The characteristic velocity of the eddies scales as $\left(zF_B\right)^{1/3}$.

While the characteristic velocity increases slowly with altitude, the characteristic buoyancy actually decreases. Note that these solutions are only valid for $z >> z_0$.

We can also make some inferences about the ensemble mean temperature gradient. On dimensional grounds,

$$g\beta\frac{d\overline{T}}{dz} = -c_1F_B^{2/3}z^{-4/3}, \tag{2.54}$$

where c_1 is just a constant. This can be integrated in the vertical to give

$$\overline{T} = \overline{T}_0 - \frac{3c_1}{g\beta}F_B^{2/3}\left[\left(z_0^T\right)^{-1/3} - z^{-1/3}\right], \tag{2.55}$$

where we have used $\overline{T} = \overline{T}_0$ at $z = z_0^T$. The mean temperature falls off with height and approaches an asymptotic value given by

$$\overline{T}_\infty = \overline{T}_0 - \frac{3c_1}{g\beta}F_B^{2/3}\left(z_0^T\right)^{-1/3}. \tag{2.56}$$

While this simple convection problem has an elegant dimensional solution, it is difficult to test it in the laboratory. Quite apart from not being able to achieve a good approximation to an infinite Boussinesq fluid, cooling a laboratory fluid uniformly through its depth is problematic. Fortunately, in a Boussinesq system, the equations are equivalent to a system in which there is

no cooling but the boundary temperature increases linearly in time. To the author's knowledge, this has not actually been tried.

Alternatively, we can make measurements of the actual atmosphere under circumstances that approximate the idealized problem. Boundary layers over deserts can extend upward to 5 km, and one might hope that the lower portions of these, away from the boundary layer top, will not be too affected by it. Also, air is not nearly incompressible, being close to an ideal gas. Fortunately, the Boussinesq approximation can be extended by a suitable change of the temperature variable to potential temperature, θ, defined

$$\theta = T\left(\frac{p_0}{p}\right)^{R/c_p}, \tag{2.57}$$

where p_0 is a reference pressure and R is the gas constant for (dry) air. Note, by comparing (2.51) to (2.57), that *the entropy is proportional to the natural logarithm of the potential temperature*. In this case, θ (or entropy) rather than T is the adiabatic invariant of the system, and buoyancy is defined

$$B = g\frac{\theta'}{\overline{\theta}}, \tag{2.58}$$

where the prime denotes a fluctuation away from the mean state, denoted by the overbar. The Boussinesq approximation can be shown to be valid in this case for convective layer depths much smaller than the density scale height of the atmosphere, which is roughly 8 km. Thus boundary layers extending to 5 km over deserts do not satisfy the Boussinesq approximation very well.

A far more serious problem, however, is that close to the surface, most of the turbulence kinetic energy is generated mechanically by wind flowing over terrain rather than by convection. We shall return to this problem in Chapter 4. For now we will look at observations in a location with very strong surface heating and weak ambient winds. Figure 2.13 shows measurements of potential temperature over a desert during the middle of the day, made using an instrumented model airplane. The red dots show potential temperature in air moving upward while the blue dots are for downward moving air. The magenta curve is a solution of a relation formed by combining (2.55) and (2.56) and using potential rather than absolute temperature:

$$\overline{\theta} = \theta_0 - \left(\theta_0 - \overline{\theta}_\infty\right)\left(1 - \left(\frac{z_0^T}{z}\right)^{1/3}\right). \tag{2.59}$$

We plot the solution for $T_0 = 330\ K,\ \overline{T}_\infty = 316.2\ K,$ and $z_0^T = 0.01\,m.$ To be sure, this is a weak test of the theory, but both the observations and the theory show that, except in a very thin layer near the surface, *dry convection produces a mean state in which the potential temperature is nearly constant with height*. (When there is significant variability of water vapor concentration, as in the tropical atmosphere, we must modify this statement to account for the effect of water vapor on specific volume. In Chapter 3 we show that accounting for this, in the absence of phase change of water convection produces a mean state in which the *virtual* potential temperature is constant with height.)

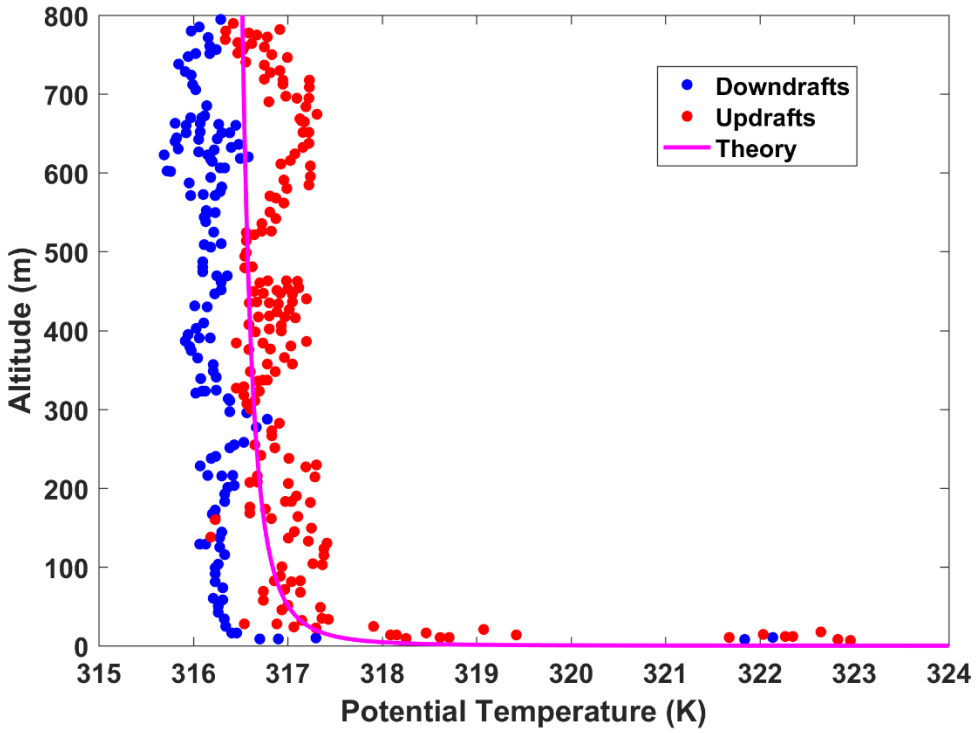

Figure 2.13: Model aircraft measurements of potential temperature during a sunny day over a desert near Albuquerque, New Mexico, on 3 August 1993. Red dots show upward moving air; blue dots show downward moving air. Magenta curve shows the theoretical solution (2.55) with $T_0 = 330\ K,\ z_0^T = 0.01\ m,$ *and* c_1 *chosen so that* $\overline{T}_\infty = 316.2\ K$.

While this elegant and simple problem illustrates some of the most fundamental features of dry convection, real tropical boundary layers are strongly influenced by the presence of mean winds, which in practice drive much of the turbulence near the surface. We shall discuss this in much more detail in Chapter 3. We shall see that the general statement that (virtual) potential temperature tends to be constant with altitude in convecting boundary layers remains true even in the presence of mean wind. For now we make use of this observation to illustrate dry convective-radiative equilibrium.

2.4 Dry convective-radiative equilibrium

We next turn to a model of dry convective turbulence in statistical equilibrium with radiative forcing. Fundamentally, we have to add convective heat transfer to radiative transfer, making sure also to account for convective transfer from the surface to the atmosphere.

One way to think about this is to recognize, from Figure 2.11, that radiation tries to drive the atmosphere to a state that is unstable to dry convection in much of the troposphere. Convection, on the other hand, transports enthalpy upward, trying to restabilize the atmosphere. This tug-of-war results in a statistical equilibrium state in which the sum of the radiative (including solar) and convective fluxes vanishes at each altitude.

But this is far from an equal competition, because in our atmosphere, the time scale for perturbations to relax back to radiative equilibrium is much larger than the time it takes convection to erase entropy gradients.

Let's try to develop characteristic time scales for relaxation to radiative equilibrium and to convective neutrality.

For radiation, we will return to our simple gray-body model given by (2.29) – (2.31). We will start with the equilibrium solution given by (2.34) – (2.36) and add infinitesimal temperature perturbations to it, denoted here by primes. The change in enthalpy at a given altitude is just the convergence of the net flux of energy:

$$\rho c_p \frac{\partial T'}{\partial t} = -\frac{\partial F}{\partial z} = -\frac{\partial \tau_\nu}{\partial z}\frac{\partial F}{\partial \tau_\nu} = -\frac{\partial \tau_\nu}{\partial z}\left(-U' - D' + 8\sigma \bar{T}^3 T'\right), \tag{2.60}$$

where $\bar{T}$ is the radiative equilibrium temperature (which is a function of τ_ν). In deriving the right side of (2.60) we used (2.29) and (2.32), linearizing about the equilibrium state and assuming that the absorption coefficient is not a function of temperature. Now eliminating U' and D' using the linearized versions of (2.30) and (2.31) yields

$$\left(\frac{\partial^2}{\partial \tau_\nu^2} - 1\right)\left(\frac{\partial p}{\partial \tau_\nu}\frac{c_p}{g}\frac{\partial T'}{\partial t}\right) = \frac{\partial^2}{\partial \tau_\nu^2}\left(8\sigma \bar{T}^3 T'\right). \tag{2.61}$$

Here we have also used hydrostatic balance: $\frac{\partial \tau_\nu}{\partial z} = -\rho g \frac{\partial \tau_\nu}{\partial p}$. We are not going to actually solve (2.61) but rather use it to get an estimate of the radiative relaxation time scale. Suppose the temperature perturbations oscillate quasi-sinusoidally over a characteristic optical depth $\Delta\tau_\nu$. We also neglect the time dependence of the lower boundary condition, equivalent to assuming that the surface temperature is fixed. Then it follows from (2.61) that a characteristic time scale for radiative relaxation is

$$t_{rad} \cong \frac{c_p\left(1 + \left(\Delta\tau_\nu\right)^2\right)}{8\sigma g \bar{T}^3 \frac{-\partial \tau_\nu}{\partial p}}. \tag{2.62}$$

Clearly the shortest time scales will be associated with temperature perturbations that vary rapidly with altitude, so that $\Delta\tau_\nu << 1$. For these, and calculating $\partial\tau_\nu / \partial p$ from (2.40), we get

$$t_{rad} \cong \frac{c_p p_0}{8\sigma g \bar{T}^3 \tau_{\nu\infty}}. \tag{2.63}$$

For our atmosphere, this time scale is around 5 days. At the opposite limit, when the perturbations vary over long optical depths, the time scale would be around 35 days. (Later we will show that the characteristic radiative relaxation time scale in a moist atmosphere is somewhat longer, and if the surface temperature is also calculated, longer still.)

By contrast, a characteristic convective adjustment time scale is just the time it takes a turbulent plume to traverse the depth, H, of an unstable layer. This is just H divided by a characteristic vertical velocity scale. For the simple convection problem we solved earlier, this vertical velocity scale is $\left(F_b H\right)^{1/3}$, so the characteristic time scale is $\left(H^2 / F_B\right)^{1/3}$. For typical values of the buoyancy flux and depth, this is a few hours, roughly two orders-of-magnitude faster than the radiative relaxation time. Thus in our atmosphere, in the competition between radiation and convection, the convection "wins" and the equilibrium state is much closer to convective neutrality than to radiative equilibrium. We expect radiative-dry convective equilibrium to be characterized by nearly constant (virtual) potential temperature.

For this reason, the simplest conceivable way to account for convective heat transfer within the atmosphere is simply to adjust the profile of potential temperature to a constant wherever radiation forces it to decrease with altitude. We assume no external energy sources operate during the adjustment, so that the total energy content of the column is invariant during the adjustment. We assume that any kinetic energy generated by the convection is locally dissipated back into enthalpy, thus the mass-weighted vertical integral of the enthalpy must remain constant during the adjustment. So if the layer between pressure levels p_1 and p_2 has decreasing potential temperature, θ, then it would be adjusted so that

$$\theta_{new} = c + \frac{1}{p_2 - p_1}\int_{p_1}^{p_2} \theta_{old}\, dp', \tag{2.64}$$

where c is a constant determined so that enthalpy is conserved during the adjustment:

$$\int_{p_1}^{p_2} c_p T_{new}\, dp' = \int_{p_1}^{p_2} c_p T_{old}\, dp'. \tag{2.65}$$

The adjustment will of course increase the potential temperature at the top of the initially unstable layer, and decrease it at the bottom. In so doing, it may cause the potential temperature to decrease between the top of the initially unstable layer and the air just above it, and/or between the air just below the layer and the base of the layer. So these will have to be adjusted as well. In general, this *dry adiabatic adjustment* is an iterative process.

The thermodynamic disequilibrium between the surface and the air in contact with it, a general feature of radiative equilibrium, will give rise to a convective heat flux from the surface to the atmosphere, further altering the equilibrium state. In the case of pure convection, if we know the surface temperature and the potential temperature away from the surface, we can turn (2.56) around algebraically and model the surface buoyancy flux (which is proportional to the surface heat flux in a dry atmosphere) as

$$F_B = \left[\frac{g}{3c_1\theta_s}\left(\theta_s - \bar{\theta}_a\right)\right]^{3/2}\left(z_0^T\right)^{1/2}, \tag{2.66}$$

where θ_s is the surface potential temperature, $\bar{\theta}_a$ is the ensemble mean potential temperature some distance above the surface, and we have made use of the fact that the coefficient of thermal expansion of an ideal gas is its inverse temperature. But as discussed in the next chapter, turbulence near the surface is dominated by shear production when even a weak wind

is present, and in cases where shear production dominates, the heat flux from the surface is better modelled as

$$F_s = C_k \rho \, |\bar{\mathbf{V}}| \left(T_s - \bar{T}_a \right), \tag{2.67}$$

where C_k is a dimensionless transfer coefficient that depends on surface roughness but is of order 10^{-3}, ρ is the near-surface air density, $|\bar{\mathbf{V}}|$ is the ensemble mean speed of the horizontal wind a short distance above the surface, T_s is the surface temperature, and $\bar{T}_a$ is the ensemble mean air temperature a short distance above the surface.

To illustrate the profound effect of convection on the equilibrium state, we will apply dry convective adjustment to the same radiative model used to produce Figures 2.11 and 2.12, and use (2.67) with a fixed wind speed of $5\, ms^{-1}$ to calculate surface sensible heat flux into the atmosphere. The fixed relative humidity profile is the same as was used in the calculation of pure radiative equilibrium. The result is shown by the magenta curve in Figure 2.14 and compared with both a mean tropical sounding (dashed blue curve) and the pure radiative equilibrium solution (solid blue curve). The magenta and blue dots at the bottom show the calculated sea surface temperatures in the two cases.

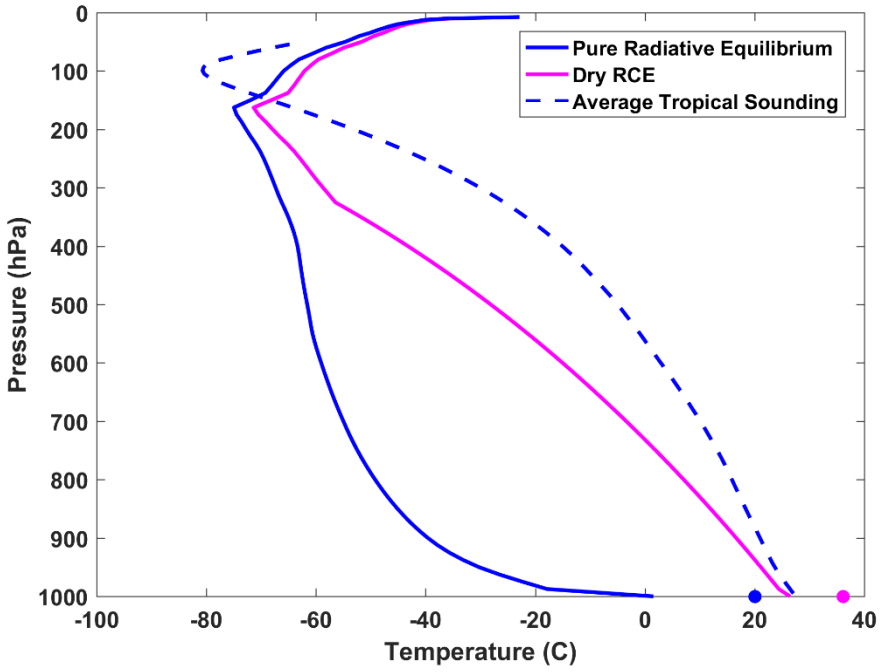

Figure 2.14: Radiative-dry convective equilibrium (magenta curve) calculated using dry convective adjustment and surface fluxes given by (2.67). This is compared to the pure radiative equilibrium solution (solid blue) and mean tropical temperature profile (dashed blue). The magenta and blue dots at the bottom show the calculated sea surface temperatures for the adjusted and pure radiative cases, respectively.

The temperature profile is dry adiabatic up to about 300 hPa and the whole profile is considerably warmer, and closer to the tropical mean sounding, than the pure radiative equilibrium solution. The surface temperature is close to 36^{o} C, considerably warmer than the pure radiative equilibrium solution and much warmer than observed sea surface temperatures in the tropics, which peak at around 30^{o} C. The tropopause and the lower stratosphere are a bit warmer than the pure radiative equilibrium solution.

The addition of a turbulent heat flux from the surface to the atmosphere cools the surface and heats the atmosphere; this is the main reason that the adjusted profile is warmer that the pure radiative equilibrium solution. This effect is amplified by water vapor feedback: The warmer state, under the assumption of constant relative humidity, has more water vapor – an important greenhouse gas. Thus the system warms further.

Note that heat transfer from the surface reduces but does not eliminate the temperature jump between the surface and the atmosphere.

Figure 2.15 shows the rates of radiative and dry convective heating in equilibrium, expressed as degrees of temperature change per day. In equilibrium, the two must sum to zero and so they are mirror images of each other. The strong turbulent heat flux from the surface to the atmosphere causes so much warming that the whole troposphere up to about 300 hPa cools radiatively, at a remarkably constant rate of roughly $1.5\,K\,day^{-1}$, though a bit larger close to the surface.

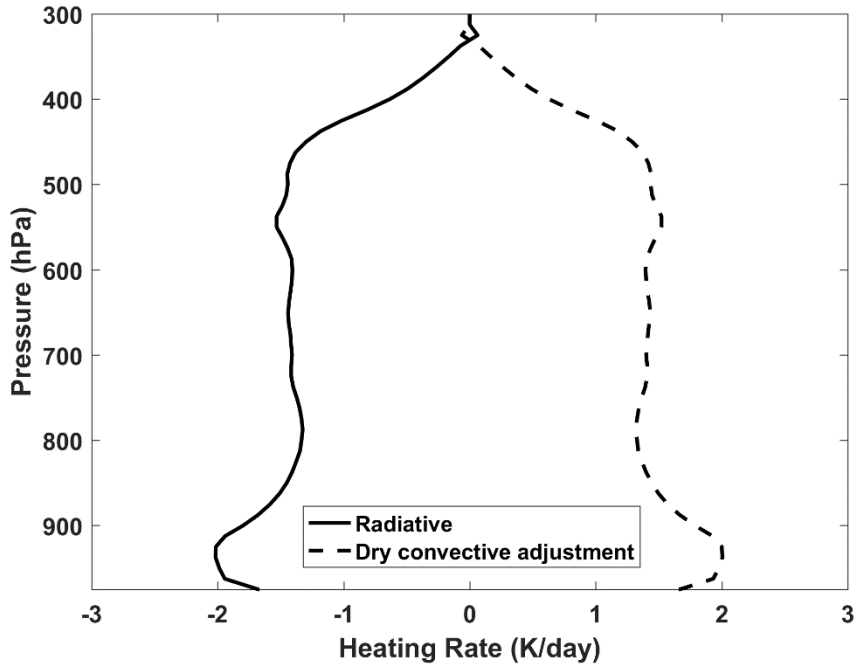

Figure 2.15: Radiative (solid) and convective (dashed) heating rates in the radiative-dry convective equilibrium solution corresponding to Figure 2.14.

In reality, dry convection would rapidly homogenize the mass concentration of water (specific humidity) through the convecting layer, likely producing clouds in the upper part of the layer and thereby radically altering the radiative transfer. Nonetheless, the equilibrium state illustrated in Figures 2.14 and 2.15 serves to contrast the pure radiative equilibrium with a convectively adjusted equilibrium and sets the stage for the real problem, moist convection.

2.5 Moist RCE, Part I

The dynamics and physics of the tropical atmosphere are made vastly richer by phase changes of water. Most of these phase changes occur within cumulus and cumulonimbus clouds, whose presence is much of what makes tropical skyscapes so beautiful. Water plays a dual role: latent heat released and absorbed when water changes phase makes a first-order contribution to atmospheric thermodynamics, and at the same time, water in all its phases has a strong effect on radiative transfer. As we shall see, this makes even relatively simple problems like radiative-convective equilibrium daunting, but far richer and more interesting than their dry counterpart. Our currently incomplete understanding of moist convection makes tropical meteorology still something of a frontier subject in atmospheric science and climate.

The subject of moist convection is far too broad and deep to treat in anything like a comprehensive way in a book that attempts to cover the landscape of tropical meteorology; all we can do here is review some essential elements. In my years of teaching tropical meteorology at the graduate level I have found that dislodging cherished but flawed concepts developed at the undergraduate level more challenging than conveying wholly new material.

One false conception that is particularly difficult to dislodge is the idea that large-scale tropical circulations are driven by latent heat release. This idea is widely expressed in textbooks and in research literature. In the field of tropical cyclones this is expressed in the notion that such storms are driven by latent heat release within the deep cumulonimbi that surround the cyclone center. This idea is just as false as the statement that elevators are driven by counterweights, and for the same essential reason. It fails to recognize that convection in the one case, and the transmission of tension through steel cables in the other, are fast processes, and that the system dynamics are rate-limited by slower processes….radiation and surface enthalpy fluxes in the tropical atmosphere and the electric motor in the case of the elevator. We will begin by illustrating this point with a simple example. But first, we review some essential points about the thermodynamics and microphysics of moist convection:

1. Condensation and evaporation of cloud condensate are nearly reversible processes. The very small super saturations needed for heterogeneous nucleation ensure that, except in rare circumstances, supersaturations are very small and water vapor and cloud condensate may be considered to be in thermodynamic equilibrium with each other.

2. For this reason, condensation and evaporation can be considered internal processes that can best be handled by a redefinition of the adiabatic invariants of the system. They should not be treated in the same way as external heat sources and sinks. (This is not the case, however, for evaporation of precipitation, which is not usually a thermodynamic equilibrium process.)

3. The exotic nature of moist convection is therefore not owing to phase change per se but to key irreversible processes: the formation, fallout, and partial or total re-evaporation of precipitation, and mixing across sharp gradients of water concentration.

To illustrate these points, we consider a variation on the very simple convection problem we considered in section 2.3. In this variation, we take the atmosphere to be saturated with respect to water vapor, and filled with cloud, such that the total water mass concentration per unit mass of dry air, r_t (also called the total water *mixing ratio*) is constant. We do not allow any precipitation or flux of water through the lower boundary, so that r_t is a locally conserved variable. As in the original problem, we cool the atmosphere and keep the surface temperature fixed, so that the whole system is turbulently convecting, and this turbulent convection thoroughly mixes the total water concentration, which consequently is constant. Temperature will be decreasing with height, and thus, according to the Clausius-Clapeyron equation, the saturation vapor pressure decreases with height. Thus as we ascend, more and more of the total water concentration is in the form of cloud, and less and less in the form of vapor. This is illustrated by the shading in Figure 2.16.

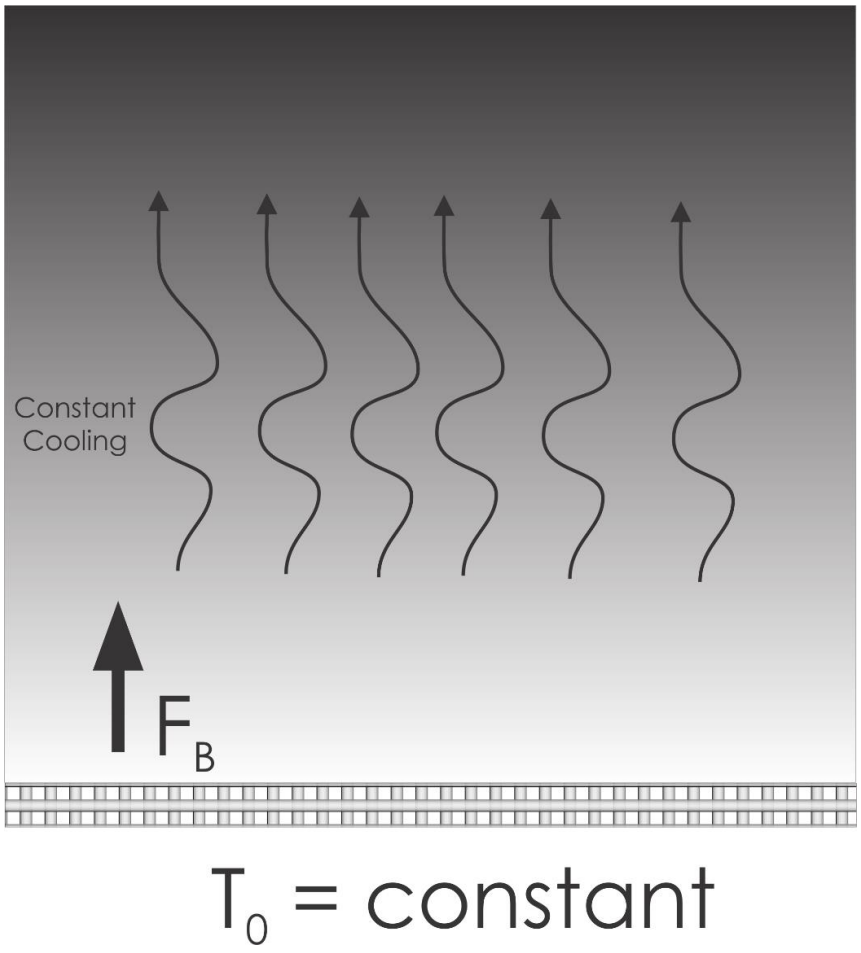

Figure 2.16: As in Figure 2.12 but for a water-saturated atmosphere with constant total water concentration, but whose cloud water content (shading) increases with altitude.

For this inhomogeneous gas, any state variable may be expressed as a function of any other *three* state variables (as opposed to two for homogeneous systems). Thus, if we like, we can express the specific volume as a function of the system entropy, pressure, and total water mixing ratio:

$$\alpha = \alpha\left(s, p, r_t\right), \tag{2.68}$$

where here the entropy, s, is the entropy of a mixture of dry air, water vapor, and liquid water. (We ignore the ice phase here.) This may be written (e.g. see Emanuel, 1994) as

$$s = \left(c_{pd} + r_t c_l\right)\ln(\frac{T}{T_0}) - R_d \ln(\frac{p_d}{p_0}) + \frac{L_v r}{T} - r R_v \ln(\mathcal{H}) + c_l r_t, \tag{2.69}$$

where c_{pd} is the heat capacity at constant pressure of dry air, c_l is the heat capacity of liquid water, r is the mixing ratio (mass of water vapor per unit mass of dry air), r_t is the total water mixing ratio (mass per unit mass of dry air), R_d is the gas constant for dry air, p_d is the partial pressure of dry air, L_v is the latent heat of vaporization, R_v is the gas constant for water vapor, and $\mathcal{H}$ is the relative humidity, defined as the ratio of actual to saturation vapor pressure. As we may add arbitrary constants to the definition of entropy, we have included reference temperature and pressure, T_0 and p_0, and also added the very last term which is a function of another conserved variable; this makes what follows more compact. In our problem, the air is always saturated – the relative humidity is 1 – and so the second to last term in (2.69) is absent.

Using the chain rule, we can write perturbations to the specific volume, at constant pressure, as

$$\alpha' = \left(\frac{\partial \alpha}{\partial s}\right)_{p,r_t} s', \tag{2.70}$$

remembering that the total water concentration is constant in the problem. Now, as in the dry case, we can develop a Maxwell relation from the definition of specific enthalpy, which for a mixture of dry air, water vapor, and liquid water may be written (Emanuel, 1994):

$$k = \left(c_{pd} + r_t c_l\right)T + L_v r. \tag{2.71}$$

By differentiating (2.69) and (2.71), we can show that

$$dk = Tds - c_l T \ln(\frac{T}{T_0})dr_t + \alpha\left(1 + r_T\right)dp. \tag{2.72}$$

By applying to (2.72) the following identity:

$$\left(\frac{\partial}{\partial s}\right)_{p,r_t}\left(\frac{\partial k}{\partial p}\right)_{s,r_t} = \left(\frac{\partial}{\partial p}\right)_{s,r_t}\left(\frac{\partial k}{\partial s}\right)_{p,r_t}, \tag{2.73}$$

we arrive at the desired Maxwell relation:

$$\left(\frac{\partial \alpha}{\partial s}\right)_{p,r_t} = \frac{1}{1+r_t}\left(\frac{\partial T}{\partial p}\right)_{s,r_t}, \tag{2.74}$$

which is practically identical to the dry case (2.45) except for the different definition of entropy and the factor $1+r_t$, which is close to unity in our atmosphere. From (2.70), the buoyancy, defined by (2.48), is then

$$B = \frac{\Gamma_m}{1+r_t} s', \tag{2.75}$$

where $\Gamma_m = -\left(\frac{\partial T}{\partial z}\right)_{s,r_t}$ is the *moist adiabatic lapse rate*. This is very similar to the dry case (2.49) except for the different definition of entropy, the $1+r_t$ factor, and the moist rather than dry adiabatic lapse rate.

It is important to note that the moist adiabatic lapse rate varies with altitude, in contrast to the dry adiabatic lapse rate, which is a constant, assuming that the acceleration of gravity does not vary much over the depth of the convecting layer. Thus, according to (2.75), for a given entropy fluctuation, the buoyancy will vary depending on the altitude and it is no longer the case that the buoyancy flux is related to the heat flux by a fixed constant. Thus it would appear that the dimensional reasoning we used to deduce how various quantities vary with altitude in the dry case will not work for the present case, because there is an additional non-constant parameter, Γ_m.

To see the problem, let's look at the equation for the time mean, horizontally averaged turbulence kinetic energy. This is formed by representing all the quantities (velocities, buoyancy, and pressure) by the sum of a time mean, horizontally averaged component plus a fluctuating part. Symbolically, for any variable v,

$$v = \overline{v}(z) + v'(x, y, z, t). \tag{2.76}$$

We apply this decomposition to all the variables, substitute them into the Boussinesq equations, and form from them an equation for the kinetic energy. We then take the time and horizontal averages of this equation. Neglecting the molecular diffusion terms, as we did in the dry case, the result is

$$\frac{\partial}{\partial z}\left[\overline{w'^3} + \alpha_0 \overline{p'w'}\right] = \overline{w'B'} = \frac{\Gamma_m}{1+r_t}\overline{w's'}, \tag{2.77}$$

where, as a result of the Boussinesq approximation, α_0 is a representative (constant) value of the specific volume and the overbars represent time and horizontal means. The far right side of (2.77) uses (2.75) for the buoyancy. Now to within the Boussinesq approximation, the convective heat flux, F, is just $T_0\overline{w's'}$, where T_0 is a representative temperature. Thus we may write (2.77) as

$$\frac{\partial}{\partial z}\left[\overline{w'^3}+\alpha_0\overline{p'w'}\right]=\frac{\Gamma_m F}{(1+r_t)T_0}. \tag{2.78}$$

The problem is that the right side of (2.78) varies with altitude and so we no longer have a one-parameter problem. However, we can reduce this back to a problem involving a single constant parameter by defining a new vertical coordinate, μ, that is linear in absolute temperature, rather than altitude, but has the same dimensions as altitude:

$$\mu \equiv \frac{T_0-\overline{T}}{\Gamma_d}. \tag{2.79}$$

Here $\overline{T}$ is the absolute temperature along a moist adiabat (that is, a curve of constant entropy). We have from this that

$$\frac{\partial}{\partial z}=\frac{\partial}{\partial \mu}\frac{\partial \mu}{\partial z}=\frac{\Gamma_m}{\Gamma_d}\frac{\partial}{\partial \mu}. \tag{2.80}$$

Applying (2.80) to (2.78) transforms the latter to

$$\frac{\partial}{\partial \mu}\left[\overline{w'^3}+\alpha_0\overline{p'w'}\right]=\frac{\Gamma_d F}{(1+r_t)T_0}\equiv F_B. \tag{2.81}$$

Now the right had side is a constant, which we will call F_B, and we are back to a one parameter problem. All the conclusions that we reached in the dry case apply to this case as well, with a very slightly different definition of F_B and with the alternative vertical coordinate defined by (2.79). Among these conclusions are

4. The characteristic size of the turbulent eddies scales with the modified altitude μ above the surface.
5. The characteristic buoyancy of the eddies scales as $F_B^{2/3}\mu^{-1/3}$.
6. The characteristic velocity of the eddies scales as $(\mu F_B)^{1/3}$.

Note from (2.80) that quantities vary more slowly with z than they do with μ, because $\Gamma_m < \Gamma_d$. For a surface temperature of 30 ºC, the variations with z would be only about 1/3 as fast as variations with μ, but traveling upward into lower temperatures, the moist adiabatic lapse rate increases and asymptotically approaches the dry adiabatic lapse rate. Thus for low surface temperatures or in the upper troposphere, μ is essentially equivalent to z.

It can be seen from this simple example that the phase change of water does not materially change convection. Moist convection behaves pretty much like dry convection. One can always revert to a description of this system in terms of dry entropy (or potential temperature), in which case the thermodynamic equation would have large sources and sinks owing to condensation and evaporation. One could say that thermals are driven upward by latent heat release and downward by absorption of latent heat, but this would be a clumsy way of describing it. In

general, dynamical systems are described most compactly and intuitively by using the most conserved variables available.

What makes real moist convection *qualitatively* different from dry convection is not latent heat release per se, but rather the strongly irreversible processes of the fall of precipitation and its re-evaporation into unsaturated air.

Suppose now that, in our simple convecting system, a demon removes condensed water as soon as it forms, so that while upward moving air is generally saturated, it contains a very small amount of condensed water (just enough to make the condensate visible as cloud). A slight downward displacement, by warming the sample, renders it unsaturated. Thus, broadly speaking, most upward moving air is saturated and experiences latent heat release, while most downward moving air is unsaturated. The form the convection takes is illustrated by Figure 2.17.

Figure 2.17: Configuration of clouds in an atmosphere in which a uniform cooling is imposed above a liquid water surface held at fixed temperature. A demon removes condensed water as soon as it forms, leaving just enough to render the saturated air visible as cloud.

The upward-moving saturated air, were it not for mixing, would follow a *pseudo-adiabatic* lapse rate of temperature. This is a defined by a process in which displaced air remains saturated, but any condensate that forms is removed. Condensate therefore does not contribute to the effective buoyancy of the air, nor does it contribute to it heat capacity. Since at each step the system's state is defined uniquely by its temperature and pressure (with its water vapor content determined by Clausius-Clapeyron), it is possible to define a pseudo-entropy that is exactly conserved in a pseudo-adiabatic process. Although it is not possible to derive an exact closed-form expression for the pseudo entropy, an empirical expression valid over the observed range of tropospheric temperature and pressure was developed by Bolton (1980). He chose to express it in terms of a temperature-like variable called the pseudo *equivalent potential temperature*, θ_{ep} , whose logarithm is proportional to the pseudo entropy:

$$\theta_{ep} = T\left(\frac{1000}{p}\right)^{0.2854(1-0.28r)} \times \exp\left[r(1+0.81r)\left(\frac{3376}{T^*} - 2.54\right)\right], \tag{2.82}$$

where r is the mixing ratio and T^* is the *saturation temperature*; that is, the temperature at which air becomes saturated when displaced adiabatically. This is accurate to within 0.3 K for tropospheric conditions. Note that θ_{ep} is always larger than θ and that $\lim_{r\to 0} \theta_{ep} = \theta$; the pseudo-equivalent potential temperature asymptotically approaches ordinary potential temperature as the mixing ratio vanishes.

Since pseudo-entropy is a function of temperature and pressure alone when the air is saturated (and thus the mixing ratio, r, is at is saturated value, which is itself a function of temperature and pressure alone), lines of constant saturation pseudo-entropy, usually referred to as *moist adiabats*, can be graphed on a thermodynamic diagram, as shown in Figure 2.18.

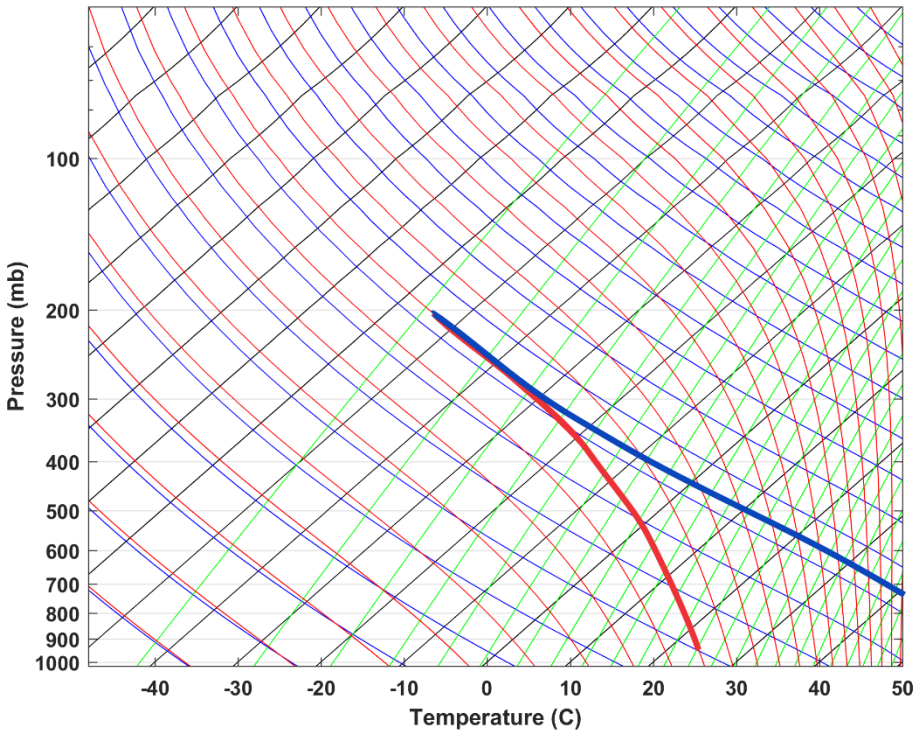

Figure 2.18: A typical atmospheric thermodynamic diagram. This particular format is known as a Skew-T-log-p diagram, because isotherms run diagonally rather than vertically (so that typical atmospheric temperature profiles are more erect). Pressure forms the ordinate, at equal intervals of the logarithm of the pressure. The blue curves are dry adiabats (curves of constant θ) and the red curves are pseudo- moist adiabats (curves of constant θ_{ep}). Curves of constant saturation mixing ratio are shown in green. The heavy red lines shows an example of saturated, pseudo-adiabatic ascent from 950 hPa and 25 °C to 200 hPa while the heavy blue curve illustrates dry adiabatic descent.

The particular thermodynamic diagram illustrated in Figure 2.18 is called a *Skew-T* diagram because isotherms run diagonally rather than vertically; this is done so that typical atmospheric temperature profiles are more vertical. Pressure forms the ordinate, at equal intervals of the logarithm of the pressure. The blue curves are dry adiabats (curves of constant θ) and the red curves are pseudo- moist adiabats (curves of constant θ_{ep}). Curves of constant saturation mixing ratio are shown in green.

Suppose we consider a sample of air that is saturated at 25 ^{o}C and 950 hPa and lift it by a pseudo-adiabatic process to 200 hPa. This is shown by the heavy red line in Figure 2.18. Now take that air and increase its pressure without adding or subtracting energy. Because it never has any condensed water in it, there is no evaporation, and the sample descends dry adiabatically, as shown by the thick blue curve in Figure 2.18.

Note that the descending air is warmer than the ascending air, so that the rising air is negatively buoyant with respect to the descending air. This process would convert kinetic to potential energy and so would not happen spontaneously. (Were the air to descend all the way back down to 950 hPa, its temperature would be 88 ^{o}C; the difference between this and the starting temperature of the sample reflects the latent heat added to the sample during its ascent.)

Thus there is a problem with the picture of moist RCE shown by Figure 2.17. For the descending air to have a temperature equal to or lower than that of the ascending stream, it must lose energy, and in reality it does so by radiative cooling. Observations, which we shall review in the next section, show that there is in fact very little difference between the temperature of the ascending and descending streams, and that the temperature profile in the clouds is not far from moist adiabatic. The thermodynamic balance in the descending air is then

$$c_p \rho w_e \frac{T}{\theta} \frac{d\theta}{dz} = \dot{Q}_{rad}, \tag{2.83}$$

where w_e is the vertical velocity and $\dot{Q}_{rad}$ is the rate of radiative heating in the unsaturated air. As we shall show, $\dot{Q}_{rad}$ is almost always negative, consistent with descent in between clouds. We expect that the potential temperature stratification, $d\theta / dz$, is determined by the condition that the temperature profile be nearly moist adiabatic. Thus (2.83) really determines the descent rate in the clear air, given the rate of radiative cooling.

In RCE, there can be no net mass flux through any level, otherwise the air density would be changing over time. Suppose that updrafts have a characteristic upward velocity w_c and cover a fractional area σ. Then the flux of mass through any level, which must vanish, is given by

$$\sigma \rho w_c + (1-\sigma) \rho w_e = 0. \tag{2.84}$$

For convenience, we define M to be the net upward convective mass flux per unit area:

$$M \equiv \sigma \rho w_c = -(1-\sigma) \rho w_e. \tag{2.85}$$

Observations show that $\sigma << 1$, so that $M \cong -\rho w_e$. Since the clear-air velocity is determined by the rate of radiative cooling and the potential temperature stratification along a moist adiabat, it

follows that the net upward convective mass flux is very nearly determined by these two quantities.

Note that where the convective mass flux, as given by (2.85) together with (2.83), decreases with altitude, mass must flow from the convective updrafts into the environment. Thus the water budget in the sinking air in between clouds (which occupies the majority of the volume of the system since $\sigma << 1$) is given by

$$\rho w_e \frac{dr_e}{dz} = \left(r^* - r_e \right) \mathrm{MAX}\left(-\frac{dM}{dz}, 0 \right), \tag{2.86}$$

where r_e is the mixing ratio in the clear air. If the profile of radiative cooling and the system temperature are known, then (2.83) can be solved for w_e and thus M, using (2.85), and then (2.86) can be solved for the mixing ratio of the clear air, r_e.

But note that this would require iterating through (2.83), (2.85), and (2.86) because the radiative heating rate depends strongly on the clear-air water vapor content. This illustrates the strongly nonlinear nature of moist RCE – radiative cooling drives the convection, which in turn determines the moisture of the free troposphere and thereby strongly affects the radiative cooling.

In the case of radiative cooling that is constant with altitude, (2.83) shows that w_e and thus M would increase with altitude, since the potential temperature stratification decreases upward along moist adiabats. In that case, the right side of (2.86) would be zero except for a delta function at the tropopause. Thus the mixing ratio of the whole troposphere above the subcloud layer would be equal to the saturation mixing ratio of the tropopause. Given that tropical tropopause temperatures are around -70 ^{o}C, this would be miniscule, and the relative humidity would thus be close to zero except very close to the tropopause. This is very far from what is observed in the tropics, or what is produced by numerical simulations of idealized moist RCE states, about which more in due course.

Since in the real world, radiative cooling profiles are roughly constant with altitude in the troposphere, the excessive dryness of solutions to (2.86) is likely not owing to the lack of convective detrainment but almost certainly to our extreme assumption that all condensed water is removed from the system. This strong, highly artificial sink of water is responsible for the excessive dryness of the solution to (2.86). We must modify our simple picture of RCE to include the microphysics governing precipitation formation, fall, and re-evaporation.

So we revise the conceptual picture of RCE of Figure 2.17 to include formation, fallout, and partial re-evaporation of precipitation, as shown in Figure 2.19. Saturated air ascends with mass flux M_u and re-evaporation of falling precipitation drives downward motion of mostly unsaturated air with mass flux M_d. We here redefine the “clear air” as the slowly subsiding air outside both the clouds and the unsaturated downdrafts. If we define the total convective mass flux as M and the “clear air” as excluding both the cloud and rain areas, then (2.83) and (2.85) apply as with the pseudo-adiabatic case.

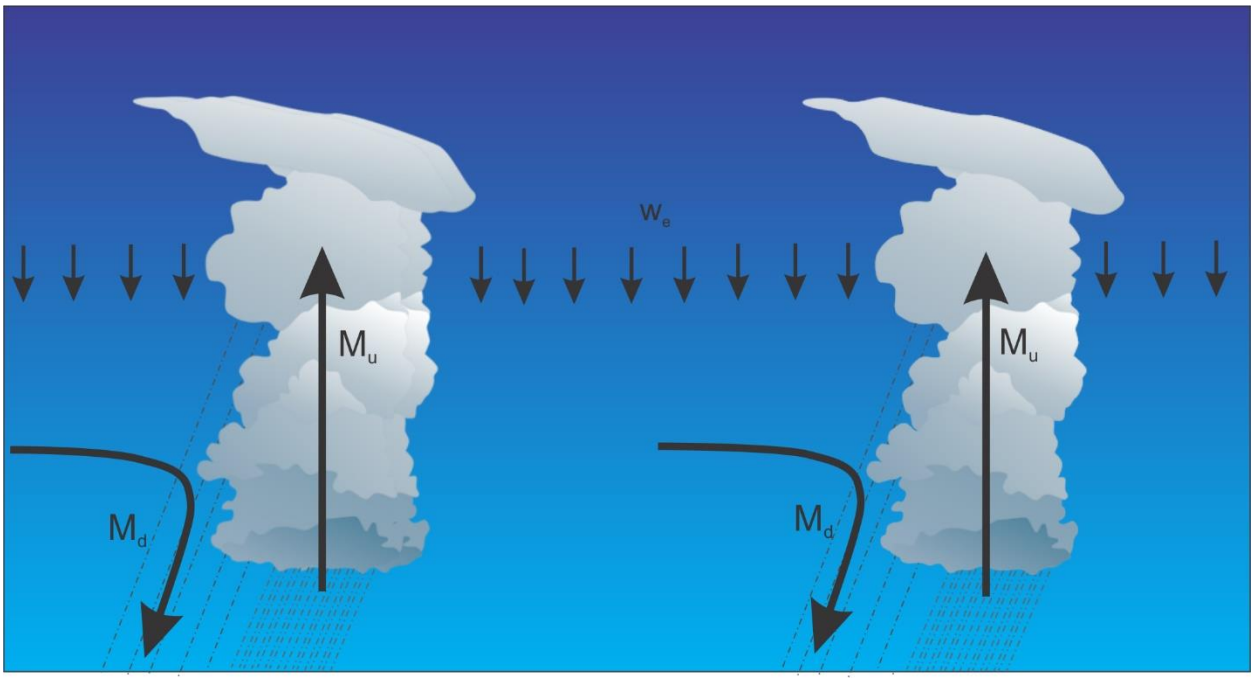

Figure 2.19: Moist RCE with precipitation. Broadly, saturated air ascends with mass flux M_u and re-evaporation of falling precipitation drives downward motion of mostly unsaturated air with mass flux M_d. We here redefine the "clear air" as the slowly subsiding air outside both the clouds and the unsaturated downdrafts.

Rather than focus on the water budget of just the clear air, we will look at the flux of water through each level across the whole system. That flux must vanish, since in equilibrium water cannot accumulate above any level. This condition is given by

$$M\left(r_t - r_e\right) - P = 0, \tag{2.87}$$

where r_t is the total water mixing ratio (including cloud water) inside the clouds, and P is the total downward precipitation flux through the level in question. Rearranging this and using (2.85) for M under the approximation that $\sigma << 1$ gives

$$r_e = r_t - \frac{P}{\rho w_e}, \tag{2.88}$$

with ρw_e given by (2.83). This shows that the humidity of the clear air is governed by the microphysics that determine how much cloud water exists at a given level (which sets the amount by which r_t exceeds r^*) and how much precipitation is formed. More cloud water yields a moister environment, while more precipitation dries the environment.

We can make this more intuitive with a simple example. Suppose that a fixed fraction ϵ_p of water condensed at any level is converted to precipitation, and that another fixed fraction, ϵ_r of the precipitation evaporates before reaching the level in question. The precipitation flux through any level z is then given by

$$P = -\left(1-\epsilon_r\right)\int_z^{z_t} \epsilon_p M \frac{dr^*}{dz} dz, \tag{2.89}$$

where z_t is the altitude of the clouds tops. The integrand in (2.89) is just the precipitation formation efficiency multiplied by the rate of condensation. Again using (2.85) with $\sigma << 1$ and substituting (2.89) into (2.88) gives

$$r_e = r_t + \frac{\left(1-\epsilon_r\right)}{\rho w_e}\int_z^{z_t} \epsilon_p \rho w_e \frac{dr^*}{dz} dz. \tag{2.90}$$

One interesting special case of (2.90) is the case of ρw_e and ϵ_p constant with height, in which case (2.90) reduces to

$$r_e = r_t - \left(1-\epsilon_r\right)\epsilon_p \left(r^* - r(z_t)\right). \tag{2.91}$$

Note that we can recover the pseudo-adiabatic limit by setting $\epsilon_r = 0$, $\epsilon_p = 1$, and $r_t = r^*$. In that case, $r_e = r(z_t)$ as before.

The relation (2.91) shows that the smaller the efficiency ϵ_p with which precipitation is formed, and the greater the re-evaporation of precipitation ϵ_r, the moister the environment. Note that smaller precipitation efficiency will also elevate the cloud water content, and thus the total water mixing ratio r_t.

Thus, unequivocally, the humidity of the clear air in RCE is set by cloud microphysical and radiative processes. The rate of radiative cooling and the ambient potential temperature stratification along a moist adiabat, which together determine ρw_e, enter in a more subtle way. Note that if we simply multiply the radiative cooling everywhere by a constant factor, that factor cancels in (2.90) and there is no effect on the environmental mixing ratio. (However, the system temperature will be different, thus altering the relative humidity.) From (2.90) we can conclude that, all other things being equal, if the radiative subsidence ρw_e increases in magnitude with altitude above the level in question, the air will be drier, whereas if it decreases with altitude, the air will be moister. Always remember that the water vapor content strongly influences the radiative cooling rate, so that ρw_e depends on water. Moreover, the vapor content outside convective clouds is important in the formation of stratiform clouds, which themselves strongly affect radiative transfer in both the visible and infrared, so the actual problem of moist RCE is a strongly two-way process, with the radiation and surface fluxes driving the convection and the latter lofting water from its source of the surface and thereby influencing radiative transfer by altering the vapor and cloud water profiles outside the convective clouds themselves.

We will return to a detailed treatment of moist RCE in the following section. But next we turn to the topic of moist convection itself.

References

Bolton, D., 1980: The computation of equivalent potential temperature. *Mon. Wea. Rev.*, **108,** 1046-1053.

Emanuel, K. A., 1994: *Atmospheric convection.* Oxford Univ. Press, New York, 580 pp., translator.

Nicolis, G., and I. Prigogine, 1977: *Self-organization in nonequilibrium systems.* John Wiley & Sons, New York, 490 pp., translator.

Pierrehumbert, R. T., 2010: *Principles of planetary climate.* Cambridge University Press, New York, 652 pp., translator, 978-0-521-86556-2.